

World Journal of *Radiology*

World J Radiol 2024 July 28; 16(7): 241-293



EDITORIAL

- 241 Advantages of the intradermal lymphoscintigraphy
Tartaglione G

ORIGINAL ARTICLE**Retrospective Study**

- 247 Ultrasomics in liver cancer: Developing a radiomics model for differentiating intrahepatic cholangiocarcinoma from hepatocellular carcinoma using contrast-enhanced ultrasound
Su LY, Xu M, Chen YL, Lin MX, Xie XY

- 256 Correlation between dose-volume parameters and rectal bleeding after 12 fractions of carbon ion radiotherapy for prostate cancer
Ono T, Sato H, Miyasaka Y, Hagiwara Y, Yano N, Akamatsu H, Harada M, Ichikawa M

Observational Study

- 265 Incidence of exclusive extrapelvic skeletal metastasis in prostate carcinoma on bone scintigraphy
Singh P, Agrawal K, Rahman A, Singhal T, Parida GK, Gnanasegaran G

SYSTEMATIC REVIEWS

- 274 Evaluating the role of 7-Tesla magnetic resonance imaging in neurosurgery: Trends in literature since clinical approval
Perera Molligoda Arachchige AS, Meuli S, Centini FR, Stomeo N, Catapano F, Politi LS

ABOUT COVER

Editorial Board Member of *World Journal of Radiology*, Ali Abbasian Ardakani, PhD, Assistant Professor, Department of Radiology Technology, School of Allied Medical Sciences, Shahid Beheshti University of Medical Sciences, Tehran 1971653313, Iran. ardakani@sbmu.ac.ir

AIMS AND SCOPE

The primary aim of *World Journal of Radiology* (*WJR*, *World J Radiol*) is to provide scholars and readers from various fields of radiology with a platform to publish high-quality basic and clinical research articles and communicate their research findings online.

WJR mainly publishes articles reporting research results and findings obtained in the field of radiology and covering a wide range of topics including state of the art information on cardiopulmonary imaging, gastrointestinal imaging, genitourinary imaging, musculoskeletal imaging, neuroradiology/head and neck imaging, nuclear medicine and molecular imaging, pediatric imaging, vascular and interventional radiology, and women's imaging.

INDEXING/ABSTRACTING

The *WJR* is now abstracted and indexed in PubMed, PubMed Central, Emerging Sources Citation Index (Web of Science), Reference Citation Analysis, China Science and Technology Journal Database, and Superstar Journals Database. The 2024 Edition of Journal Citation Reports® cites the 2023 journal impact factor (JIF) for *WJR* as 1.4; JIF without journal self cites: 1.4; 5-year JIF: 1.8; JIF Rank: 132/204 in radiology, nuclear medicine and medical imaging; JIF Quartile: Q3; and 5-year JIF Quartile: Q3.

RESPONSIBLE EDITORS FOR THIS ISSUE

Production Editor: *Xin-Xin Che*, Production Department Director: *Xu Guo*; Cover Editor: *Jia-Ping Yan*.

NAME OF JOURNAL

World Journal of Radiology

ISSN

ISSN 1949-8470 (online)

LAUNCH DATE

January 31, 2009

FREQUENCY

Monthly

EDITORS-IN-CHIEF

Thomas J Vogl

EDITORIAL BOARD MEMBERS

<https://www.wjgnet.com/1949-8470/editorialboard.htm>

PUBLICATION DATE

July 28, 2024

COPYRIGHT

© 2024 Baishideng Publishing Group Inc

INSTRUCTIONS TO AUTHORS

<https://www.wjgnet.com/bpg/gerinfo/204>

GUIDELINES FOR ETHICS DOCUMENTS

<https://www.wjgnet.com/bpg/GerInfo/287>

GUIDELINES FOR NON-NATIVE SPEAKERS OF ENGLISH

<https://www.wjgnet.com/bpg/gerinfo/240>

PUBLICATION ETHICS

<https://www.wjgnet.com/bpg/GerInfo/288>

PUBLICATION MISCONDUCT

<https://www.wjgnet.com/bpg/gerinfo/208>

ARTICLE PROCESSING CHARGE

<https://www.wjgnet.com/bpg/gerinfo/242>

STEPS FOR SUBMITTING MANUSCRIPTS

<https://www.wjgnet.com/bpg/GerInfo/239>

ONLINE SUBMISSION

<https://www.f6publishing.com>

Evaluating the role of 7-Tesla magnetic resonance imaging in neurosurgery: Trends in literature since clinical approval

Arosh S Perera Molligoda Arachchige, Sarah Meuli, Francesca Romana Centini, Niccolò Stomeo, Federica Catapano, Letterio S Politi

Specialty type: Radiology, nuclear medicine and medical imaging

Provenance and peer review: Invited article; Externally peer reviewed.

Peer-review model: Single blind

Peer-review report's classification

Scientific Quality: Grade C

Novelty: Grade B

Creativity or Innovation: Grade B

Scientific Significance: Grade C

P-Reviewer: Yu RQ

Received: April 6, 2024

Revised: May 8, 2024

Accepted: June 17, 2024

Published online: July 28, 2024

Processing time: 108 Days and 12.6 Hours



Arosh S Perera Molligoda Arachchige, Sarah Meuli, Francesca Romana Centini, Faculty of Medicine, Humanitas University, Pieve Emanuele, Milan 20072, Italy

Niccolò Stomeo, Department of Anaesthesiology and Intensive Care, IRCCS Humanitas Research Hospital, Via Manzoni 56, Rozzano, Milan 20089, Italy

Niccolò Stomeo, Federica Catapano, Letterio S Politi, Department of Biomedical Sciences, Humanitas University, via Rita Levi Montalcini 4, 20090 Pieve Emanuele - Milan, Italy

Federica Catapano, IRCCS Humanitas Research Hospital, Via Manzoni 56, 20089 Rozzano - Milan, Italy

Letterio S Politi, Department of Neuroradiology, IRCCS Humanitas Research Hospital, Via Manzoni 56, Rozzano, Milan 20089, Italy

Corresponding author: Letterio S Politi, MD, Professor, Department of Biomedical Sciences, Humanitas University, Via Rita Levi Montalcini 4, Pieve Emanuele, Milan 20072, Italy. letterio.politi@hunimed.eu

Abstract

BACKGROUND

After approval for clinical use in 2017, early investigations of ultra-high-field abdominal magnetic resonance imaging (MRI) have demonstrated its feasibility as well as diagnostic capabilities in neuroimaging. However, there are no to few systematic reviews covering the entirety of its neurosurgical applications as well as the trends in the literature with regard to the aforementioned application.

AIM

To assess the impact of 7-Tesla MRI (7T MRI) on neurosurgery, focusing on its applications in diagnosis, treatment planning, and postoperative assessment, and to systematically analyze and identify patterns and trends in the existing literature related to the utilization of 7T MRI in neurosurgical contexts.

METHODS

A systematic search of PubMed was conducted for studies published between January 1, 2017, and December 31, 2023, using MeSH terms related to 7T MRI and neurosurgery. The inclusion criteria were: Studies involving patients of all ages, meta-analyses, systematic reviews, and original research. The exclusion criteria

were: Pre-prints, studies with insufficient data (*e.g.*, case reports and letters), non-English publications, and studies involving animal subjects. Data synthesis involved standardized extraction forms, and a narrative synthesis was performed.

RESULTS

We identified 219 records from PubMed within our defined period, with no duplicates or exclusions before screening. After screening, 125 articles were excluded for not meeting inclusion criteria, leaving 94 reports. Of these, 2 were irrelevant to neurosurgery and 7 were animal studies, resulting in 85 studies included in our systematic review. Data were categorized by neurosurgical procedures and diseases treated using 7T MRI. We also analyzed publications by country and the number of 7T MRI facilities per country was also presented. Experimental studies were classified into comparison and non-comparison studies based on whether 7T MRI was compared to lower field strengths.

CONCLUSION

7T MRI holds great potential in improving the characterization and understanding of various neurological and psychiatric conditions that may be neurosurgically treated. These include epilepsy, pituitary adenoma, Parkinson's disease, cerebrovascular diseases, trigeminal neuralgia, traumatic head injury, multiple sclerosis, glioma, and psychiatric disorders. Superiority of 7T MRI over lower field strengths was demonstrated in terms of image quality, lesion detection, and tissue characterization. Findings suggest the need for accelerated global distribution of 7T magnetic resonance systems and increased training for radiologists to ensure safe and effective integration into routine clinical practice.

Key Words: 7-Tesla; Magnetic resonance imaging; Neuroimaging; Neurosurgery; Pathologies; Procedures; Trends

©The Author(s) 2024. Published by Baishideng Publishing Group Inc. All rights reserved.

Core Tip: Frequent neurosurgical procedures using 7-Tesla magnetic resonance imaging (7T MRI) include endoscopic neurosurgery, resective epilepsy surgery, and deep brain stimulation, addressing conditions like cerebrovascular diseases, epilepsy, pituitary adenoma, and gliomas. Leading in publications are the United States, Netherlands, South Korea, and Japan. 7T MRI enhances the understanding of neurological and psychiatric disorders, showing superiority in image quality, lesion detection, and tissue characterization, underscoring the need for global deployment and improved radiologist training.

Citation: Perera Molligoda Arachchige AS, Meuli S, Centini FR, Stomeo N, Catapano F, Politi LS. Evaluating the role of 7-Tesla magnetic resonance imaging in neurosurgery: Trends in literature since clinical approval. *World J Radiol* 2024; 16(7): 274-293

URL: <https://www.wjgnet.com/1949-8470/full/v16/i7/274.htm>

DOI: <https://dx.doi.org/10.4329/wjr.v16.i7.274>

INTRODUCTION

In the realm of modern medicine, the field of neurosurgery stands as a testament to the remarkable progress achieved through advancements in technology and imaging. The delicate and intricate nature of the human brain necessitates tools and techniques that allow for precise diagnosis, treatment planning, and surgical intervention. Among the many innovations that have revolutionized the field, one technology has emerged as a promising game-changer: The 7-Tesla magnetic resonance imaging (7T MRI) scanner which received United States FDA approval for clinical use in 2017[1-3]. The introduction of 7T MRI represents a pivotal moment in the history of neurosurgery. This remarkable imaging technology harnesses the power of ultra-high magnetic fields to produce images with unprecedented detail and resolution, far surpassing the capabilities of conventional magnetic resonance imaging (MRI) scanners[4]. By capitalizing on the inherent magnetic properties of hydrogen nuclei within the human body, 7T MRI offers both neurosurgeons and neurologists an invaluable tool to investigate deeper into the intricate structures of the brain, enabling them to make more precise assessments of pathologies and formulate optimized treatment strategies[5,6]. Traditionally, neurosurgery has relied upon lower field strength MRI machines, typically operating at 1.5 or 3 T. While these systems have been instrumental in guiding surgical interventions and aiding in preoperative planning, they often fall short in providing the level of detail required for complex neurosurgical cases[2,3]. The limitations of lower field strength MRI, such as reduced spatial resolution and limited contrast, have posed challenges in accurately delineating critical structures, identifying subtle abnormalities, and characterizing lesions, ultimately affecting the quality and safety of neurosurgical procedures[5,6]. The emergence of 7T MRI, with its higher magnetic field strength, has raised the bar for neuroimaging capabilities. It promises to unveil new dimensions of information that were previously concealed, shedding light on intricate anatomical details and subtle pathologies that were once elusive[5,6]. This newfound precision has the potential to redefine the landscape of neurosurgery by offering enhanced preoperative assessment and surgical guidance, ultimately leading to improved patient outcomes and reduced surgical risks. This systematic review aims to systematically analyze and

identify patterns and trends within the existing literature on the utilization of 7T MRI in neurosurgical contexts, focusing on its applications in the diagnosis, treatment planning, and postoperative assessment of various neurosurgically treated pathologies.

MATERIALS AND METHODS

A systematic search of the PubMed database was conducted to identify relevant studies published between January 1, 2017 and December 31, 2021, using the following MeSH search terms: ((7T MRI) AND (neurosurgery)). Two independent reviewers performed the initial search and screening, with the inclusion criteria encompassing studies involving patients of all ages (both pediatric and adults) where 7-T MRI imaging was performed and/or compared with conventional MRI imaging in the context of neurosurgery. Eligible study types included meta-analyses, systematic reviews, and original research. The exclusion criteria involved studies with insufficient data such as case reports, publications not in English, and studies of animal subjects. Data synthesis involved standardized extraction forms. Our objective was to analyze trends in the literature as well as to provide a comprehensive and descriptive overview of research conducted within the specified time frame. Given the nature of our research question and the scope of our analysis, we chose not to perform a formal risk of bias assessment for individual studies using QUADAS or Rob2[7-9]. Our decision was based on the recognition that our aim was to capture and summarize the breadth of research in this field rather than to make judgments about the quality or internal validity of the included studies, nor the determination of diagnostic accuracy. Despite not having assessed study bias, we do acknowledge that it is a potential issue. Nonetheless, we have reported key characteristics and methodological details of the studies in our analysis, including any notable limitations or methodological considerations, to provide readers with a transparent understanding of the included literature. Note that no complex statistical methods were employed in this study as the research was descriptive in nature and focused on summarizing the usage patterns and clinical applications of 7T MRI in neurosurgery. **Table 1** summarizes the studies falling under each pathology discussed, their primary endpoints, and 7T MRI sequences used.

RESULTS

We initially identified a total of 219 records from the PubMed database within our defined period. We found no duplicate publications or any other reason to remove any manuscript before screening. All 219 articles were screened and out of them 125 were excluded as they did not meet our inclusion criteria. Finally, 94 reports were retrieved and 2 out of them were irrelevant to neurosurgery, and 7 were animal studies. This yielded a total of 85 studies that were included in our systematic review (**Figure 1**). We manually categorized the data in our database to obtain the number of publications available on PubMed for each of the neurosurgical procedures discussed in them as well as for each neurosurgically treated disease. According to our data, the most common neurosurgical procedures utilizing 7-T MRI were endoscopic neurosurgery, resective epilepsy surgery, and deep brain stimulation (DBS) surgery. **Figure 2** illustrates publications (p) per each procedure. The most treated pathologies were cerebrovascular diseases (10p), followed by epilepsy (8p), pituitary adenoma (7p), and gliomas (12p). However, it should be noted that under cerebrovascular diseases, a series of diseases were considered, such as amyloid angiopathy (1p), arteriovenous malformations (1p), stroke (2p), atherosclerosis (1p), intracranial aneurysms (4p), and intracerebral hemorrhage (ICH) (1p) (**Figure 3**). We also sorted the number of publications produced by each country. For this, only the institutional affiliation of the first author was considered. The countries with the highest absolute number of publications were the United States (27p) followed by the Netherlands (16p), South Korea (15p), Japan (13p), and Germany (7p) (**Figure 4**). In addition, we also present the number of 7T MRI facilities in each country (**Figure 5**). We also noticed that there has been a decline in the research output in the year 2018 and in 2022 (**Figure 6**). The experimental studies included were classified into comparison studies if 7T MRI was compared with lower field strengths, typically 1.5T and 3T, and into non-comparison studies (**Figure 7**).

DISCUSSION

Through the analysis of the included articles, several important observations and implications have emerged. The use of 7T MRI has demonstrated great potential in improving the characterization and understanding of various neurological and psychiatric conditions such as temporal lobe epilepsy (TLE), pituitary adenoma, unruptured intracranial aneurysms (UIAs), and movement disorders and has reported valuable insights into disease mechanisms, anatomical abnormalities, and functional alterations.

Epilepsy

7T MRI was proven to be a valuable non-invasive tool for evaluating subtle structural changes in the hippocampus of patients with TLE[10]. Specifically, the enhanced visualization of hippocampal internal architecture (HIA) can be achieved with 7T MRI. Notably, HIA asymmetry serves as a substantial predictor of the laterality of seizure onset in TLE patients, demonstrating comparable predictive efficacy to hippocampal volume asymmetry[11]. Similarly, significant advantages of using 7T MRI with post-processing techniques for identifying subtle focal cortical dysplasia lesions have been demonstrated (including increased detection rates) in patients with pharmaco-resistant epilepsy with non-lesional

Table 1 Summary of studies included in the review falling under each neurosurgically treated pathology

| Pathology | Ref. | Aim of the study | Applied 7T MRI protocol |
|-------------------|-----------------------------|---|---|
| Epilepsy | Stefanits <i>et al</i> [10] | To correlate noninvasive, high-resolution, morphological 7T MRI of the hippocampus in temporal lobe epilepsy (TLE) patients with histopathological findings | T2-weighted (T2w) 2D fast spin echo (FSE) sequence, obtained in paracoronal, hippocampal plane perpendicular to the central sulcus (matrix, 688 × 688; field of view (FOV), 230 × 172.5; image resolution, 0.33 mm × 0.33 mm × 1.5 mm; slices, 25; parallel imaging, 2; repetition time (TR), 4500 milliseconds (ms); echo time (TE), 81 ms) with an acquisition time of 8 min 48 s |
| | Wang <i>et al</i> [12] | To assess the clinical value of <i>in vivo</i> structural 7T MRI and its post-processing in patients with pharmaco-resistant epilepsy who underwent presurgical evaluation and had a nonlesional 3T MRI scan | A standard epilepsy protocol was used with the following sequences on a 7T MRI scanner (Magnetom, Siemens, Erlangen, Germany) with a head-only circularly polarized transmit and 32-channel phased array receive coil (Nova Medical, Wilminuteston, MA): 3D T1-MP2RAGE: Sagittal acquisition, TR/TE = 6000/3 ms, TI1/TI2 = 700/2700 ms, flip angle (FA) 1/FA 2 = 4°/5°, 0.75 mm isotropic-voxel resolution, 208 slices, total acquisition time (TA) = 9 min 32 s; 2D T2-GRE (spoiled-gradient echo): Axial and oblique coronal acquisition, TR/TE = 2290/17.8 ms, FA = 23°, in-plane resolution = 0.38 mm × 0.38 mm, slice thickness = 1.5 mm, 60 slices, no gap, TA = 9 min 50 s; 2D FLAIR: Axial and oblique coronal acquisition, TR/TE = 9000/124 ms, TI = 2600 ms, in-plane resolution = 0.75 mm × 0.75 mm, slice thickness = 2 mm, 45 slices, 30% gap, TA = 3 min 2 s; 3D susceptibility weighted imaging (SWI) (included only for selected cases such as vascular malformation): TR/TE = 23/15 ms, FA = 20°, voxel size = 0.49 mm × 0.49 mm × 0.8 mm, 144 slices, TA = 8 min 16 s. Two dielectric calcium titanate pads with passive B1 shimming were used to improve the signal loss in the temporal lobes |
| | Rutland <i>et al</i> [15] | To perform hippocampal subfield-specific tractography and quantify connectivity of the subfields in MRI-negative patients. Abnormal connectivity of the hippocampal subfields may help inform seizure focus hypothesis and provide information to guide surgical intervention | Participants were scanned under an Institutional Review Board-approved protocol using a 7T whole body scanner. A SC72CD gradient coil was used (Gmax = 70 mT/m, max slew rate = 200 T/m/s), with a single channel transmit and 32 channel receive head coil. The MRI scan included a T1-weighted MP2RAGE sequence: TR = 6000 ms, TE = 3.62 ms, FA = 5°, FOV = 240 mm × 320 mm, slices = 240, 0.7 mm ³ isotropic resolution, scan time = 7 min 26 s. A coronal-oblique T2w turbo spin echo sequence was included: TR = 6900 ms, TE = 69 ms, FA = 150°, FOV = 202 mm × 202 mm, in-plane resolution 0.4 mm × 0.4 mm, slice thickness = 2 mm, slices = 40, time = 6 min 14 s. A high-angular-resolved diffusion-weighted imaging (HARDI) dMRI sequence was also performed with whole-brain coverage: <i>b</i> = 1200 s/mm ² , TR = 7200 ms, TE = 67.6 ms, 1.05 mm isotropic resolution, in-plane acceleration R = 3 (GRAPPA), reversed phase encoding in the AP and PA direction for paired acquisition in 68 directions, with a TA of 20 min |
| | Veersema <i>et al</i> [13] | To determine whether the use of 7T MRI in clinical practice leads to higher detection rates of focal cortical dysplasias in possible candidates for epilepsy surgery | 7T MRI parameters are as follows: 3D T1w TFE: TE = 2.9 ms, TI = 1200 ms, TR = 9 ms, FA = 6°, resolution = 0.81 mm × 0.81 mm × 0.80 mm, matrix = 248 × 312 × 475, acquisition time = 9 min 34 s. 3D T2w turbo spin echo (TSE): TE = 302 ms, TR = 3200 ms, FA = 90°, resolution = 0.70 mm × 0.70 mm × 0.70 mm, matrix = 356 × 357 × 543, acquisition time = 10 min 24 s. 3D T2*w: TE = 27 ms, TR = 88 ms, FA = 24°, resolution = 0.50 mm × 0.50 mm × 0.50 mm, matrix = 480 × 381 × 600, acquisition time = 7 min 23 s; 3D MP-FLAIR: TE = 300 ms, TI = 2200 ms, TR = 8000 ms, FA = 90°, resolution = 0.80 mm × 0.82 mm × 1.00 mm, matrix = 312 × 304 × 380, acquisition time = 8 min 40 s. 3D WMS: TE = 2.0 ms, TI = 600 ms, TR = 6.73 ms, FA = 4.5°, resolution = 0.80 mm × 0.80 mm × 0.80 mm, matrix = 320 × 320 × 474, acquisition time = 8 min 42 s |
| | Zhang <i>et al</i> [11] | To compare the hippocampal internal architecture (HIA) between 3 and 7T MRI in patients with TLE | All patients underwent MRI scans with a 7 T scanner. Thirty-two channel head coils were used with both scanners. For the assessment of HIA, T2w images (T2WI) in the coronal plane located perpendicular to the long axis of the hippocampus were collected (7T T2WI-TSE): TR = 9640 ms, TE = 72 ms, resolution 0.3 mm × 0.3 mm × 2.0 mm, FA = 60°, TA = 11 min 26 s. 7T T1WI 3D-magnetization prepared rapid acquisition gradient echo (3D-MPRAGE): TR = 2200 ms, TE = 2.98 ms, resolution = 0.7 mm × 0.7 mm × 0.7 mm, FA = 8°, TA = 10 mi 16 s |
| | Sharma <i>et al</i> [14] | To quantitatively assess surgical outcomes in epilepsy patients who underwent scanning at 7T whose lesions were undetectable at conventional field strengths (1.5T/3T) | Unspecified |
| | van Lanen <i>et al</i> [16] | To assess whether 7T MRI increases the sensitivity to detect epileptogenic lesions | N/A (systematic review) |
| Pituitary adenoma | Yao <i>et al</i> [18] | To examine the utility of 7T MRI in predicting the tumor consistency of pituitary adenomas | High-resolution 7T TSE (0.4 mm × 0.4 mm × 2 mm), MP2-RAGE (0.75 mm isotropic), and TOF (0.26 mm × 0.26 mm × 0.4 mm) acquisitions on all patients |
| | Rutland <i>et al</i> [20] | To investigate microstructural damage caused by pituitary macroadenomas by performing probabilistic tractography of the optic tracts and | Participants were scanned under an Institutional Review Board-approved protocol using a 7T whole body scanner. A SC72CD gradient coil was used (Gmax = 70 mT/m, max slew rate = 200 T/m/s), with a single channel transmit and 32-channel receive head coil. Scanning included a T1-weighted |

| | | |
|---------------------------|---|--|
| | radiations using 7T diffusion-weighted MRI (DWI). These imaging findings were correlated with neuro-ophthalmological results to assess the utility of ultra-high-field MRI for objective evaluation of damage to the anterior and posterior visual pathways | MP2RAGE sequence with the following parameters: TE (ms) = 5.1, TR (ms) = 6000, TI (ms) = 1050 (3000), FA = 5° (4°), FOV = 240 mm × 320 mm, slices = 240, resolution = 0.7 mm isotropic, scan time = 7 min 26 s. Quantitative T1-maps were derived from the MP2RAGE sequence. A coronal-oblique T2-TSE (TE = 69, TR = 6900, FA = 150°, FOV = 202 mm × 202 mm, in-plane resolution 0.4 mm × 0.4 mm, slice thickness = 2 mm, slices = 40, time = 6 min 14 s) and HARDI dMRI ($b = 1200 \text{ mm}^2/\text{sec}$, TE = 67.6, TR = 7200, resolution = 1.05 mm isotropic, in-plane acceleration R = 3 (GRAPPA), reversed phase encoding in AP and PA directions for paired acquisition in 68 directions, TA = 20) sequences were acquired |
| Rutland <i>et al</i> [21] | To leverage ultra-high-field 7T MRI to study the retinotopic organization of the primary visual cortex (V1) and correlate visual defects with cortical thinning in V1 to characterize consequences of pituitary adenomas on the posterior visual system | Participants were scanned using a 7T whole-body scanner (Magnetom, Siemens Healthineers). A SC72CD gradient coil was used (Gmax = 70 mT/m, maximum slew rate = 200 T/m/sec), with a single-channel transmit and 32-channel receive head coil (Nova Medical). Scanning included a T1-weighted MP2RAGE sequence with the following parameters: TE = 3.62 ms, TR 6000 ms, TI = 1050 ms (2 nd pulse 3000 ms), FA = 5° (2 nd pulse 4°), FOV = 224 mm × 168 mm, number of slices = 240, voxel size = 0.7 mm isotropic, and scan time = 8 min 8 s. Coronal oblique T2w turbo spin echo (TE = 59 ms, TR = 6000 ms, FA = 180°, FOV = 200 mm × 168 mm, in-plane voxel size = 0.4 mm × 0.4 mm, slice thickness = 2 mm, number of slices = 60, time = 6 min 50 s) and high-angular-resolved DWI ($b = 1200 \text{ mm}^2/\text{s}$, TE = 67.6 ms, TR = 7200 ms, voxel size = 1.05 mm isotropic, FA = 180°, number of slices = 66, in-plane acceleration R = 3, reversed-phase encoding in anteroposterior and posteroanterior directions for paired acquisition in 64 directions, TA = 18 min 38 s) sequences were prescribed. Dielectric pads and localized shimming methods were employed to reduce signal artifact at the skull base |
| Patel <i>et al</i> [22] | To describe the initial experience using ultra-high-field 7T MRI in patients with suspected Cushing's disease and negative or equivocal imaging at conventional field strengths | Patients were scanned on a Siemens Terra 7T system using a Nova Medical 1Tx/32Rx head coil. Pre- and post- contrast (0.2 mL/kg gadoterate megluminutense) T1-weighted pituitary sequences included coronal and sagittal 2D TSE (TR = 960 ms, TE = 10 ms, voxel size = 0.2 mm × 0.2 mm × 2.0 mm), 3D SPACE (TR = 1200 ms, TE = 12 ms, variable FA, voxel size = 0.5 mm × 0.5 mm × 0.5 mm), and 3D MPRAGE (TR = 2300 ms, TE = 2.95 ms, FA = 7°, voxel size = 0.7 mm × 0.7 mm × 0.7 mm). Not all patients were scanned with all sequences due to changes in clinical protocol during the study period |
| Rutland <i>et al</i> [23] | To examine 7T DWI as a novel method of measuring the consistency of pituitary adenomas | Participants were scanned using a 7T whole-body scanner. A SC72CD gradient coil was used (Gmax = 70 mT/m, maximum slew rate = 200 T/m/s), with a single-channel transmit and 32-channel receive head coil. Scanning included a T1-weighted MP2RAGE sequence with the following parameters: TE = 3.62 ms, TR = 6000 ms, TI = 1050 ms (2 nd pulse 3000 ms), FA = 5° (2 nd pulse 4°), FOV = 224 mm × 168 mm, number of slices = 240, voxel size = 0.7 mm isotropic, and scan time = 8 min 8 s. Coronal oblique T2w turbo spin echo (TE = 59 ms, TR = 6000 ms, FA = 180°, FOV = 200 mm × 168 mm, in-plane voxel size = 0.4 mm × 0.4 mm, slice thickness = 2 mm, number of slices = 60, time = 6 min 50 s) and high-angular-resolved DWI ($b = 1200 \text{ mm}^2/\text{s}$, TE = 67.6 ms, TR = 7200 ms, voxel size = 1.05 mm isotropic, FA = 180°, number of slices = 66, in-plane acceleration R = 3, reversed-phase encoding in anteroposterior and posteroanterior directions for paired acquisition in 64 directions, TA = 18 min 38 s) sequences were prescribed. Dielectric pads and localized shimming methods were employed to reduce signal artifact at the skull base |
| Rutland <i>et al</i> [24] | To determine the efficacy of 7T MRI in identifying radiological markers for endocrine function | The Institutional Review Board-approved protocol employed a 7T whole-body MRI scanner (Magnetom, Siemens Healthcare, Erlangen, Germany) with a SC72CD gradient coil (Gmax = 70 mT/m, max slew rate = 200 T/m/s), and used a single channel transmit and 32-channel receive head coil (Nova Medical, Wilminutestgon, MA, United States). Sequences included a T1-weighted MP2RAGE[14] sequence: TE (ms) = 3.62, TR (ms) = 6000, TI (ms) = 1050/3000, FA = 5°/4°, FOV = 224 mm × 168 mm, slices = 240, resolution = 0.7 mm isotropic, scan time = 8 min 8 s. Quantitative T1-maps were derived from the MP2RAGE sequence. Coronal-oblique and axial T2-TSE (TE = 60 ms, TR = 6000 ms, FA = 180°, FOV = 200 mm × 168 mm, in-plane resolution 0.4 mm × 0.4 mm, slice thickness = 2 mm, slices = 60, time = 6 min 50 s) sequences were acquired. A T1-weighted MPRAGE sequence was also obtained (TE = 4.1 ms, TR = 3000 ms, TI = 1050 ms, FA = 7°, resolution = 0.7 mm isotropic, scan time = 7 min 40 s) |
| Rutland <i>et al</i> [17] | The study quantifies visualization of tumor features and adjacent skull base anatomy in a homogeneous cohort of pituitary adenoma patients comparing 7T MRI vs standard lower field MRI | Unspecified |
| Parkinson's disease | Shamir <i>et al</i> [30] To validate the clinical application accuracy of the 7T-ML method by comparing it with identification of the subthalamic nucleus (STN) based on intraoperative microelectrode recordings | Unspecified |
| Lau <i>et al</i> [27] | To integrate ultra-high-field template | Patients were scanned on a 7T scanner (Agilent, Santa Clara, California, |

| | | |
|--------------------------------|--|--|
| | data into the clinical workflow to assist with target selection in deep brain stimulation (DBS) surgical planning | United States/Siemens, Erlangen, Germany) <i>via</i> a 24-channel transmit-receive head coil array constructed in-house with a receiver bandwidth of 50 kHz. A T1w MPRAGE sequence was acquired (TR = 8.1 ms, TE = 2.8 ms, inversion time (TI) = 650 ms, FA = 11°, matrix: 256 × 512, 230 slices, resolution = 0.59 mm × 0.43 mm × 0.75 mm). Then, a T2w turbo spin-echo 3D (TR = 3D sagittal, matrix: 260 × 366, 266 slices, resolution = 0.6 mm ³ , 4 averages) was acquired. High-resolution <i>in vivo</i> templates were created by performing group-wise linear and nonlinear registration of 12 normal subjects scanned on a human 7T imager with both T1w and T2w contrasts (available for download at http://www.nitrc.org/projects/deepbrain7t/) resulting in an unbiased group nonlinear T1w average and T2w averages at submillimeter resolution |
| La <i>et al</i> [26] | To measure hippocampal subfields <i>in vivo</i> using ultra-high-field 7T MRI and determine if these measures predict episodic memory impairment in PD during life | Participants were scanned with a 7T GE Healthcare Discovery MR950 MRI whole-body scanner (GE Healthcare, Waukesha, WI) using a 32-channel radiofrequency (RF) receive head coil contained within a quadrature transmit coil (Nova Medical, Inc., Wilminutestgon, MA). Sixteen oblique coronal images oriented perpendicular to the longitudinal axis of the hippocampus were acquired with a T2w FSE sequence: TE = 47 ms; TR = 5-8 s (cardiac gated); acquired voxel size was 0.22 mm × 0.22 mm × 1.5 mm with a slice gap of 0.5 mm, interpolated by zero filling to 0.166 mm × 0.166 mm × 1.5 mm |
| Lau <i>et al</i> [27] | To integrate ultra-high-field template data into the clinical workflow to assist with target selection in DBS surgical planning | Patients were scanned on a 7T imager (Agilent, Santa Clara, California, United States/Siemens, Erlangen, Germany) <i>via</i> a 24-channel transmit-receive head coil array constructed in-house with a receiver bandwidth of 50 kHz. A T1w MPRAGE sequence was acquired (TR = 8.1 ms, TE = 2.8 ms, TI = 650 ms, FA = 11°, matrix = 256 × 512, 230 slices, resolution = 0.59 mm × 0.43 mm × 0.75 mm). Then, a T2w turbo spin-echo 3D (TR 3D sagittal, matrix: 260 × 366, 266 slices, resolution = 0.6 mm ³ , 4 averages) was acquired. High-resolution <i>in vivo</i> templates were created by performing group-wise linear and nonlinear registration of 12 normal subjects scanned on a human 7T imager with both T1w and T2w contrasts (available for download at http://www.nitrc.org/projects/deepbrain7t/) resulting in an unbiased group nonlinear T1w average and T2w averages at submillimeter resolution |
| La <i>et al</i> [26] | To measure hippocampal subfields <i>in vivo</i> using ultra-high field 7T MRI and determine if these measures predict episodic memory impairment in PD during life | Participants were scanned with a 7T GE Healthcare Discovery MR950 MRI whole-body scanner (GE Healthcare, Waukesha, WI) using a 32-channel RF receive head coil contained within a quadrature transmit coil (Nova Medical, Inc., Wilminutestgon, MA). Sixteen oblique coronal images oriented perpendicular to the longitudinal axis of the hippocampus were acquired with a T2w FSE sequence: TE = 47 ms; TR = 5-8 s (cardiac gated); acquired voxel size was 0.22 mm × 0.22 mm × 1.5 mm with a slice gap of 0.5 mm, interpolated by zero filling to 0.166 mm × 0.166 mm × 1.5 mm |
| Oh <i>et al</i> [25] | To investigate patterns in gray matter changes in patients with Parkinson's disease by using an automated segmentation method with 7T MRI | High-resolution T1-weighted 7T MRI volumes of 24 hemispheres were acquired from 12 Parkinson's disease patients. Magnetic resonance images from all subjects were acquired using a 7T MRI system (Philips Healthcare, Cleveland, OH, United States) with a 32-channel head coil (Nova Medical, Wilminutestgon, MA, United States). Three-dimensional anatomical brain scans were acquired using a magnetization-prepared rapid-acquisition gradient-echo sequence-induced T1-weighted imaging system with the following settings: TR = 4.4 ms, TE = 2.2 ms, slice thickness = 0.5 mm, in-plane resolution = 0.5 mm × 0.5 mm, matrix size = 432 × 432, number of axial slices = 432, and TA = 5 min 57 s |
| Mathiopoulou <i>et al</i> [29] | To explore whether combining 7T T2w and DWI sequences allows for selective segmenting of the motor part of the STN and, thus, for possible optimization of DBS | 7T T2w and DWI sequences were obtained, and probabilistic segmentation of motor, associative, and limbic STN segments was performed. The MR-sequences were acquired before surgery on a 3T Philips Ingenia scanner (Philips Healthcare, Best, The Netherlands): (1) 3D sagittal T1-weighted, gadolinium-enhanced (TR = 8.81 ms, TE = 4.03 ms, echo train length (ETL) = 242, FOV = 256 mm, slice thickness = 0.9 mm, scan time = 8 min); (2) 3D axial T2w (TR = 2500 ms, TE = 230 ms, ETL = 133, FOV = 250 mm, slice thickness = 1.1 mm, scan time = 3 min); and (3) DWI (TR = 8234 ms, TE = 96 ms, <i>b</i> = 1200 s/mm ² , 32 gradient directions, phase encoding anterior-posterior, no reverse encoding, FOV = 256 mm, slice thickness = 2.0 mm, scan time = 14 min). The following MR sequences were acquired on a 7T Achieva system (Philips Healthcare) using a 32 channel receive coil (Nova Medical, Wilminutestgon, MA): (1) 3D sagittal T2w with Turbo spin echo imaging (TR = 3000 ms, TE = 324 ms, ETL = 182, FOV = 250 × 250 × 190, FA = 100°, voxel size = 0.7 mm isotropic, scan duration = 7 min); and (2) DWI (TR = 6084 ms, TE = 70 ms, ETL = 59, <i>b</i> = 1000 s/mm ² , 32 directions, FOV = 140 × 177 × 110, voxel size = 1.4 mm × 1.4 mm in-plane, slice thickness = 1.5 mm, scan duration = 13 min) |
| Isaacs <i>et al</i> [28] | The study aimed to test whether optimized 7T imaging protocols result in less variable targeting of the STN for DBS compared to clinically utilized 3T images | The 7T scan was acquired with a Siemens Magnetom scanner using a 32-channel head coil at the Scannexus Centre for Neuroimaging in Maastricht. Whole brain T1w 3D images were obtained with an adapted version of the multi echo MP2RAGE (magnetization-prepared rapid gradient echo multi-echo) sequence with 0.8 mm isotropic voxel sizes and the following parameters: 208 slices, TR = 6000 ms, TE 1/2 = (2.74 ms/8.71 ms), TI 1/2 = (750 ms/29000 ms), FA 1/2 = (4°/6°), BW 1/2 = (350 Hz/Px/150 Hz/Px), ES = 13.6 ms, interleaved and single shot multi slice mode and interleaved, sagittal orientation acquisition in the anterior-posterior direction, phase partial Fourier 6/8, parallel acquisition with GRAPPA and acceleration factor |

| | | |
|--------------------------|------------------------------|--|
| | | of 3 and TA of 10 min 56 s. Where possible, dielectric pads were placed between the side of the participants head and the receiver coil to reduce B1 inhomogeneity artefacts. The T2w 3D scan was acquired with a partial volume gradient echo ASPIRE (multi-channel phase data from multi-echo acquisitions) sequence covering the subcortex with 0.5 mm isotropic voxel sizes and the following parameters: 90 slices, 16.7% slice oversampling, TR = 33 ms, TE 1-4 =(2.49 ms, 6.75 ms, 13.50 ms, 20.75 ms), FA =12°, BW 1-4 = (300 Hz/px, 300 Hz/px, 200 Hz/px, 100 Hz/px), interleaved multi slice mode, sagittal orientation acquisition in the anterior-posterior direction, slice partial Fourier 7/8, parallel acquisition with GRAPPA and acceleration factor of 2 and TA 7 min 42 s |
| Cerebrovascular diseases | Van Tuijl <i>et al</i> [34] | To gain insight into hemodynamic imaging markers of the CoW for unruptured intracranial aneurysm (UIA) development by comparing these outcomes to the corresponding contralateral artery without an UIA using 4D flow MRI |
| | Wrede <i>et al</i> [32] | To prospectively evaluate non-contrast-enhanced 7T magnetic resonance angiography (MRA) for delineation of UIAs |
| | Uwano <i>et al</i> [36] | To investigate whether OEF maps generated by magnetic resonance quantitative susceptibility mapping (QSM) at 7 T enabled detection of OEF changes when compared with those obtained with PET |
| | Uwano <i>et al</i> [37] | To examine whether whole-brain MRA at 7 T could non-invasively detect impaired CVR in patients with chronic cerebral ischemia by demonstrating the leptomeningeal collaterals |
| | Noureddine <i>et al</i> [35] | To evaluate RF-induced tissue heating around aneurysm clips during a 7T head MR examination and determine the decoupling distance between multiple implanted clips |
| | Millesi <i>et al</i> [33] | To delineate the wall of intracranial aneurysms to identify weak areas prone to rupture |
| | Koemans <i>et al</i> [38] | To investigate whether a striped occipital cortex and intragyral hemorrhage, two markers recently detected on ultra-high-field 7T MRI in hereditary cerebral amyloid angiopathy (CAA), also occur in sporadic CAA (sCAA) or non-sCAA |
| | | Participants underwent 7T MRI (Philips Healthcare, Best, The Netherlands) using a volume transmit and 32-channel receive coil (Nova Medical, Houston, United States). For this study, the Amsterdam Medical Center “PROspective Undersampling in multiple Dimensions” software patch was used, which enables a pseudospiral ky/kz-plane acquisition scheme designed for incoherent undersampling with a variable sampling density. Time-resolved 3D phase-contrast velocity maps (4D flow scan) over the cardiac cycle were acquired with the following parameters: Angulated coronal FOV 250 (feet-head) × 190 (right-left) × 20 (anterior-posterior) mm ³ , acquired resolution of 0.7 mm × 0.7 mm × 0.7 mm, repetition time/TE = 6.4/2.2, velocity encoding sensitivity 100 cm/s, FA = 15°, nominal acceleration factor 7, and 12 reconstructed cardiac phases (<i>i.e.</i> , reconstructed temporal resolution 83 ms for a heart rate of 60 bpm). Retrospective gating used a peripheral pulse unit for heartbeat detection. Acquisition duration was 10 min |
| | | Both TOF MRA (time-of-flight magnetic resonance angiography) and non-contrast-enhanced MPRAGE were used at 7 T. 32-channel Tx/Rx RF head coil, maximum amplitude of 45 mT/m, slew rate of 200 mT/m/ms. Prior to acquisition of diagnostic sequences, B0-shimming was performed using a vendor provided gradient echo sequence and algorithm. For B1-field mapping and local FA optimization, a vendor-provided spin-echo type sequence was used; after a slice selective excitation, two refocusing pulses generate a spin-echo and a stimulated echo |
| | | A 7T MRI scanner with quadrature transmission and 32-channel receive head coils was used. Source data of QSM were obtained using a 3-dimensional spoiled gradient recalled acquisition technique with the following scanning parameters: TR, 30 ms; TE, 15 ms; FA, 20°; FOV, 256 mm; acquisition matrix size, 512 × 256; slice thickness, 2 mm; number of slices, 160; reconstruction voxel size after zero-fill interpolation, 0.5 mm ³ ; and scan time, 3 min 25 s. The sections were set in the orthogonal axial plane from the level of the superior cerebellar peduncle to high convexity. Magnitude as well as real/imaginary phase images were regenerated from this acquisition. Structural images including T2WI and magnetic resonance angiography were also obtained |
| | | MRI examinations were performed with a 7T MRI scanner with a quadrature transmission and 32-channel receive head coil system. Whole-brain single-slab 3D time-of-flight MRA was performed using the following scanning parameters: TR, 12 ms; TE, 2.8 ms; FA, 12°; FOV, 22 cm; matrix size, 512 × 384; slice thickness, 0.5 mm (zero-fill interpolation); partition, 332; tilted optimized non-saturated excitation; number of excitations, 1; and acquisition time, 10 min 32 s. Subsequently, axial and coronal maximum intensity projection images were generated after skull stripping with SPM8 software. SPECT studies were performed using two scanners and iodine 123 N-isopropyl-p-iodoamphetaminutese (¹²³ I-IMP) at a resting state with the ACZ challenge, as described previously. The voxel size was 2.0 mm × 2.0 mm × 5.0 mm in scanner 1 and 1.72 mm × 1.72 mm × 1.72 mm in scanner 2. The cerebral blood flow was quantified using the ¹²³ I-IMP autoradiography method. Angiography and SPECT studies were performed within 10 d before/after the MRI examination |
| | | Unspecified |
| | | Patients underwent ultra-high-field MRI that was performed in a whole-body 7T MRI unit (Siemens Healthcare) with a gradient strength of 40 mT/m using a 32-channel transmit/receive coil. The MRI sequence performed for this study was a nonenhanced MPRAGE sequence (TR/TE 3850/3.84 ms, isotropic voxel size 0.5 mm) |
| | | T2-weighted images were obtained. MRI markers associated with small vessel disease were scored according to the Standards for Reporting Vascular changes on neuroimaging criteria |

| | | | |
|-----------------------|-----------------------------|---|--|
| | | intracerebral hemorrhage (ICH) | |
| | Dammann <i>et al</i> [40] | To compare cerebral cavernous malformations-associated cerebral venous angioarchitecture between sporadic and familial cases using 7T MRI | In all patients, SWI was performed at 7 T (Magnetom 7T; Siemens Healthcare). Susceptibility-weighted imaging sequences were established in previous work. The whole-body ultra-high-field MR system was equipped with a single-channel transmitter/32-channel receiver head coil (Nova Medical), and a gradient system capable of 45 mT/m maximum amplitude and a slew rate of 220 mT/m/ms. The SWI parameters were as follows: TE 15 ms, TR 27 ms, FA 14°, in-plane resolution (R) 250 mm × 250 mm, slice thickness 1.5 mm, and bandwidth 140 Hz/pixel. The SWI data were processed to phase, magnitude, susceptibility, and minimum intensity projection images. In addition, anatomical T1w (TR 2500 ms, TE 1.4 ms, FA 6°, 0.7 mm isotropic), T2w (TR 6000 ms, TE 99 ms, FA 29°, ST 3 mm, R 0.5 mm ²), and time-of-flight angiography (TR 20 ms, TE 4.3 ms, FA 20°, ST 0.4 mm, R 0.2 mm ²) sequences were acquired |
| | Harteveld <i>et al</i> [31] | To compare 3T and 7T MRI in visualizing both the intracranial arterial vessel wall and vessel wall lesions | For 7T MRI, a whole-body system (Philips Healthcare, Cleveland, OH, United States) was used with a 32-channel receive coil and volume transmit/receive coil for transmission (Nova Medical, Wilminuteston, MA, United States). The imaging protocol included a 3D whole-brain T1-weighted magnetisation-prepared inversion recovery turbo spin echo intracranial vessel wall sequence |
| | Jolink <i>et al</i> [39] | To assess presence and extent of contrast agent leakage distant from the hematoma as a marker of BBB disruption in patients with spontaneous ICH | 7T MRI (Philips, Best, The Netherlands) scans were acquired with a standardized protocol; 3D T2w TR/equivalent TE = 3158/60 ms; voxel size acquired: 0.70 mm × 0.70 mm × 0.70 mm, reconstructed: 0.35 × mm × 0.35 mm × 0.35 mm), 3D T1-weighted (TR/TE 4.8/2.2 ms; voxel size acquired: 1.00 mm × 1.01 mm × 1.00 mm, reconstructed: 0.66 mm × 0.66 mm × 0.50 mm), dual echo 3D T2w (TR/first TE/ second TE 20/6.9/15.8 ms; voxel size acquired: 0.50 mm × 0.50 mm × 0.70 mm, reconstructed: 0.39 mm × 0.39 mm × 0.35 mm), and 3D FLAIR images were acquired (TR/TE/TI 8000/300/2325 ms; voxel size acquired: 0.80 mm × 0.82 mm × 0.80 mm, reconstructed: 0.49 mm × 0.49 mm × 0.40 mm). A gadolinium-containing contrast agent was administered in a single intravenous injection of 0.1 mL Gadovist/kg body weight with a maximum of 10 mL Gadovist or 0.2 mL Dotarem/kg body weight with a maximum of 30 mL Dotarem. Postgadolinium FLAIR images were acquired at least 10 min after contrast injection |
| TN | Moon <i>et al</i> [42] | To determine the central causal mechanisms of TN and the surrounding brain structure in healthy controls (HCs) and patients with TN using 7T MRI | Subjects underwent MRI scans using a 7T MR system (Philips Healthcare, Cleveland, OH, United States) with a 32-channel phased-array head coil (Nova Medical, Wilminuteston, MA, United States). 3D anatomical brain scans were acquired using magnetization prepared rapid acquisition gradient echo (MP-RAGE) sequence-induced T1w imaging with the following settings: TR = 4.6 ms, TE = 2.3 ms, FA = 110°, slice thickness = 0.5 mm, in-plane resolution = 0.5 mm × 0.5 mm, matrix size = 488 × 396, number of axial slices = 320, and TA = 5 min 53 s |
| | Moon <i>et al</i> [41] | To investigate DTI parameters and the feasibility of DTI criteria for diagnosing TN | Imaging scans were acquired with a whole-body 7T MR system (Philips Healthcare, Cleveland, OH, United States) with a 16-channel receive head coil (Nova Medical, Wilminuteston, MA, United States) and volume transmit. Standard scanning protocols included T1, 3D T2-VISTA, and DTI were used to assess microstructure and pathology changes. MRI sequences were: 7T T1 anatomical images (TR = 4.6 ms, TE = 2.3 ms, FA = 110°, thickness = 0.5 mm, voxel size 0.5 × 0.5, matrix size 488 × 396); three-dimensional T2-VISTA images to confirm offending vessels (TR = 2031 ms, TE = 303 ms, FA = 90°, voxel size 0.5 × 0.5, matrix size 360 × 360); and DTI (TR = 5606 ms, TE = 63 ms, FA = 90°, thickness = 1.5 mm, voxel size 1.5 × 1.8, matrix size 140 × 107, and $b = 700 \text{ s/mm}^2$) |
| Traumatic head injury | Hütter <i>et al</i> [43] | To evaluate the possible prognostic benefits of 7T SWI of traumatic cerebral microbleeds over 3T SWI to predict the acute clinical state and subjective impairments, including health-related quality of life, after closed head injury | The MRI examinations and their methods have been described in detail in an earlier publication. The 7T SWI acquisition time was about 13 min. UHF MR examinations were performed on a 7 T whole-body research system (Magnetom 7T, Siemens Healthcare, Germany) used in combination with 32-channel radiofrequency head coils |
| MS | Chou <i>et al</i> [44] | To evaluate the sensitivity of 7T magnetization-transfer-weighted (MTw) images in the detection of white matter lesions compared with 3T FLAIR | Participants underwent MRI in the Sir Peter Mansfield Imaging Centre using a 7T Philips Achieva scanner (Philips Medical Systems, Best, the Netherlands). The scanning protocols included 3D T1-weighted MP-RAGE imaging to assist with coregistering 3T 2D-FLAIR and 7T 3D-MTw images. Acquisition parameters at 7 T were TE = 3.2 ms; TR = 6.9 ms; TI = 800 ms; FA of the TFE readout pulse = 80°; TFE factor = 240; shot-to-shot interval = 8 s; spatial resolution = 1.25 mm × 1.25 mm × 1.25 mm; FOV = 200 mm × 200 mm × 72.5 mm; reconstruction matrix = 160 × 160 × 58 mm ³ ; and TA = 2 min |
| | Choksi <i>et al</i> [45] | The study aimed to identify white matter tracts associated with the severity of neurogenic lower urinary tract dysfunction in women with MS | 7T DTI images were acquired (matrix 158 × 158, slice thickness 1.4 mm, FOV 220 cm × 220 cm ² , 64 directions, $b = 1000 \text{ s/mm}^2$, total scan time 12 min and 14 s) on a 7T Siemens MAGNETOM Terra MRI scanner with a 32-channel single transmit head coil (3T Siemens MAGNETOM Vida MRI scanner was used in two subjects with contraindications for 7T scanner) |
| | Beck <i>et al</i> [46] | The study aimed to characterize | The 7T brain scans included axial 3D MP2RAGE (0.5 mm isometric, acquired |

| | | | |
|---------------------|--------------------------------|---|--|
| | | cortical lesions by 7T T2-/T1-weighted MRI, and to determine relationship with other MS pathology and contribution to disability | four times per scan session), sagittal 3D segmented T2w echo-planar imaging (EPI; 0.5 mm isometric, acquired in two partially overlapping volumes for full brain coverage), and axial 2D T2w multi-echo GRE (0.5 mm isometric, acquired in three partially overlapping volumes for near full supratentorial brain coverage). MP2RAGE data were processed into uniform denoised images (hereafter, T1w MP2RAGE) and T1 maps using manufacturer-provided software |
| Glioma | Prener <i>et al</i> [48] | To evaluate the potential clinical implication of the use of single-voxel magnetic resonance spectroscopy (MRS) at 7 T to assess metabolic information on lesions in a pilot cohort of patients with grades II and III gliomas | Seven patients and seven HCs were scanned using the semi-localization by adiabatic-selective refocusing sequence on a Philips Achieva 7T system equipped with a two-channel volume transmit head coil with a 32-channel receiver array. A 3D FLAIR sampled in the sagittal direction was acquired with the following parameters: TR = 7342 ms; TE = 348 ms; TI = 2200 ms; acquisition voxel size = 0.7 mm × 0.7 mm × 1.4 mm; FA = 75°; refocusing acquisition voxel size = 0.7 mm × 0.7 mm × 1.4 mm; refocusing angle = 30°; scan duration = 6 min 44 s. In this study, the scan was used for MRS voxel placement, although it was also acquired as part of an additional structural imaging research protocol |
| | Yuan <i>et al</i> [49] | The goal of the study was to explore the capability on preoperatively identifying IDH status of combining a convolutional neural network and a novel imaging modality, ultra-high-field 7T chemical exchange saturation transfer (CEST) imaging | All patients underwent MRI scans within a week prior to surgery. CEST MRI was performed on a 7T MRI scanner (MAGNETOM Terra; Siemens Healthineers, Erlangen, Germany) with a prototype-developed snapshot-CEST sequence based on a 3D gradient spoiled GRE readout with a single-channel transmit/32-channel receive head coil (Nova Medical, Wilminuteston, MA, United States). The snapshot-CEST sequence parameters were TR = 3.4 ms, TE = 1.59 ms, FA = 6°, resolution = 1.6 mm × 1.6 mm × 5 mm, and GRAPPA acceleration factor = 3 with amplitudes B1 = 0.6, 0.75, and 0.9 mT. Z-spectra were sampled unevenly by 56 frequency offsets between -300 ppm and +300 ppm. The Z-spectrum data were corrected for both B0 and B1 inhomogeneities using the WASABI method and were fit pixelwise by a five-pool Lorentzian model (water, amide, aminutese, NOE, and MT) using the Levenberg-Marquardt algorithm. For CEST data co-registration, high-resolution T1 MP2RAGE (TR = 3800 ms, TI1 = 800 ms, TI2 = 2700 ms, TE = 2.29 ms, FA = 7°, and resolution = 0.7 mm isotropic) and 3D T2-SPACE (TR = 4000 ms, TE = 118 ms, and resolution = 0.67 mm isotropic) were acquired at 7 T. Routine-clinical-sequence, contrast-enhanced T1-weighted images (TR = 6.49 ms, TE = 2.9ms, FA = 8°, spatial resolution = 0.833 mm × 0.833 mm × 1 mm), were acquired at 3 T on an Ingenia MRI scanner (Koninklijke Philips N.V., Netherlands) |
| | Prener <i>et al</i> [55] | The aim of this study was to explore the difference in gross tumor volume of DLGGs delineated from 7T and 3T MRI scans | The 7T MR system was an actively shielded Philips Achieva 7T MR system (Philips Healthcare, Best, The Netherlands). Scanning protocol settings for 7T were as follows: 3D TSE-T2 (0.7 mm × 0.7 mm × 0.7 mm) (TE = 60) and 3D FLAIR (0.7 mm × 0.7 mm × 0.7 mm) (TE = 347). Scan time for 7T was as follows: 3D TSE-T2 was 10 min 30 s and 3DFLAIR was 7 min 30 s |
| | Weng <i>et al</i> [56] | The underlying prospective study aimed to compare SLOW-EPSI to established techniques at 7 T and 3 T for IDH-mutation status determination | The applied sequences were MEGA-SVS, MEGA-CSI, SLOW-EPSI, MRSI, 3D-T1-MPRAGE, 3D-T2-SPACE, and TOF-angiography. Measurements were performed on a MAGNETOM-Terra 7T MR scanner in clinical mode using a Nova 1Tx32Rx head coil. At 7 T, MEGA-SVS: TE = 75 ms, TR = 2500 ms, VOI = 30 × 30 × 30 mm ³ , averages = 64, and TA = 5 min 42 s. MEGA-CSI: TE = 75 ms, TR = 2900 ms, VOI = 70 mm × 70 mm × 20 mm, FOV = 200 × 200 × 20 mm ³ (12 × 12 matrix), averages = 1, and TA = 8 min 10 s |
| | Yuan <i>et al</i> [50] | The study aimed to evaluate the diagnostic accuracy of combining CEST imaging and MRS for predicting glioma infiltration | CEST acquisitions were performed at 7 T on an MRI scanner (MAGNETOM Terra, Siemens Healthineers, Erlangen, Germany). A prototype snapshot-CEST (optimized single-shot GRE sequence with rectangular spiral reordering) was applied (TR = 3.4 ms, TE = 1.59 ms, FA = 6°, bandwidth = 660 Hz/pixel, grappa = 3, resolution = 1.6 mm × 1.6 mm × 5 mm) |
| | Voormolen <i>et al</i> [47] | To investigate intra- and extracranial distortions in 7T MRI scans of skull-base meningioma | The 7T scan parameters of the 3-dimensional sagittal magnetization-prepared turbo field echo sequence are as follows: FOV 256 mm × 256 mm × 200 mm (matrix 256 × 256 × 200), TI 1200 ms, ETL 256 mm ³ , readout 9 ms, TE 2.0 ms, bandwidth 506.3 Hz/pixel, and FA 8°. Total imaging time: 9 min and 36 s. Prior to the acquisition at 7 T, a B0 field map was acquired |
| Psychiatric disease | Van den Boom <i>et al</i> [51] | To investigate whether people can learn to dynamically control activity of the DLPFC, a region that has been shown to be important for working memory function and has been associated with various psychiatric disorders | fMRI performed using a 7T Philips Achieva system, with a 32-channel headcoil. Functional data recorded using an EPI sequence (TR/TE: 2.0 s/25 ms, FA: 70°, 39 axial slices, acquisition matrix 112 × 112, slice thickness 2.2 mm no gap, 2.19 mm in plane resolution). A T1-weighted image was acquired for anatomy (TR/TE: 7/2.76 ms; FA: 8°; resolution 0.98 mm × 0.98 mm × 1.0 mm) |
| | Morris <i>et al</i> [52] | To use ultra-high-field 7T MT MRI to localize the LC in humans with and without pathological anxiety, with 0.4 mm × 0.4 mm × 0.5 mm resolution in a feasible scan time. In addition, to apply a computational, data-driven LC localization and segmentation algorithm to delineate LC for all | Participants were scanned using a 7T MRI scanner (Magnetom, Siemens, Erlangen, Germany) with a 32-channel head coil at the Leon and Norma Hess Center for Science and Medicine, ISMMS. Most subjects tolerated the MRI environment well. On entering the scanner, several subjects reported dizziness lasting 1-2 min, which they found tolerable. Structural T1-weighted dual-inversion magnetization prepared gradient echo (MP2RAGE) anatomical images were acquired first (TR = 4500 ms, TE = 3.37 ms, TI1 = 1000s and 3200 ms, FA = 4° and 5°, iPAT acceleration factor = 3, bandwidth = |

| | | |
|---|--|--|
| | participants. The relationships between LC volume and trans-diagnostic measures of pathological anxiety and attentional control were subsequently examined in a dimensional approach based on the RDoC initiative, reflecting evidence that pathological anxiety is a trans-diagnostic construct | 130 Hz/pixel, 0.7 mm isotropic resolution, whole brain coverage). Second, MT-MRI data were acquired with a 3-D segmented GRE readout (turbo-FLASH; TFL) preceded by a train of 20 MT pulses of amplitude with 190 V transmit, and 7-min run time |
| Zoon <i>et al</i> [53] | The study aimed to explore the connection between the location of active DBS contact points within STN subdivisions and the development of apathy in Parkinson's disease patients undergoing DBS | 22 PD patients that underwent STN DBS between January 2019 and February 2020 were divided in an apathy and non-apaty group using the change in the Starkstein Apathy Scale after 6 mo of DBS. For both groups the location of DBS electrodes was determined based on 7T MRI subthalamic network analysis, enabling visualization of the subdivisions and their projections relative to the active contact point. MDS-UPDRS III scores were included to evaluate DBS effect |
| Alper <i>et al</i> [54] | The objective of this study was to assess volumetric differences in hippocampal subfields between MDD patients globally and HCs as well as between a subset of treatment-resistant depression patients and HCs using automatic segmentation of hippocampal subfields software and ultra-high-field MRI | Thirty-five MDD patients and 28 HCs underwent imaging using 7T MRI. A 32-channel Nova Medical head coil was used to acquire brain images for segmentation. The 90-min imaging protocol included MP2RAGE (TR 6000 ms, TI1 1050 ms, TI2 3000 ms, TE 5.06 ms, voxel 0.70 mm × 0.70 mm × 0.70 mm) and T2 TSE (TR 9000 ms, TE 69 ms, voxel 0.45 mm × 0.45 mm × 2 mm) scans acquired at a coronal oblique oriented perpendicular to the long axis of the hippocampus |
| Essential tremor Purrer <i>et al</i> [57] | The aim of the study was to analyze the localization of individual lesions with respect to the VIM and the cerebello-thalamic tract | MRI images were acquired using a 7T scanner (Siemens Magnetom, Erlangen, Germany) with a 32-channel head coil. A fast MP-RAGE sequence was utilized to acquire the WMn contrast with a high isotropic resolution of 0.7 mm. The sequence parameters were TR/TI = 4000/670 ms, matrix = 364 mm × 310 mm × 240 mm, parallel imaging acceleration factor = 3, and acquisition time = 10 min 24 s. In addition, a T1-weighted MP-RAGE was acquired with the same coverage and resolution, but TR/TI = 2500/1100 ms, FA = 7°, PA = 2, TA = 5 min 33 s |

TOF: Time-of-flight; CoW: Circle of Willis; CVR: Cerebrovascular reactivity; FLAIR: Fluid-attenuated inversion recovery; dMRI: Diffusion Magnetic Resonance Imaging; OEF: Oxygen extraction fraction; ACZ: Acetazolamide; DTI: Diffusion tensor imaging; TN: Trigeminal neuralgia; MS: Multiple sclerosis; GRE: Gradient-recalled echo; MRI: Magnetic resonance imaging.

3T MRI scans[12]. This improved detection rate may play a role in identifying suitable candidates for surgery and facilitating the complete resection of epileptogenic lesions, potentially leading to postoperative freedom from seizures [13]. Nevertheless, studies based on larger cohorts are needed to confirm its predictive value in preoperative evaluation. A quantitative assessment of surgical outcomes in patients scanned at 7 T, whose lesions were undetectable at conventional field strengths, further emphasizes the clinical impact of 7T imaging, elucidating the practical implications of employing 7T MRI in improving surgical outcomes for patients with initial elusive lesions[14]. Among 16 patients studied, 7 exhibited clear epileptogenic potential on 7T imaging, while 9 had findings of a less definite nature. Remarkably, 15 out of 16 patients achieved Engel I, II, or III outcomes, denoting substantial improvement. Notably, those with definite lesions on 7T imaging had a higher rate of achieving Engel I surgical outcomes (57.1%) compared to those with less definite lesion status (33.3%). This suggests that patients initially diagnosed as MRI-negative on lower field strength scans but with clear radiological findings on 7T, corresponding to the suspected seizure onset zone, may benefit significantly from surgical intervention[14]. A recent study suggested that employing high-resolution diffusion MRI-based tractography of hippocampal subfields enabled the quantification of connectivity within the subfields in MRI-negative patients and identified abnormal connectivity patterns. This information holds promise in refining the understanding of the seizure focus hypothesis, thereby aiding in the formulation of more informed surgical strategies [15]. These findings indicate that distinct connectivity patterns exist among hippocampal subfields in different types of epilepsy, holding potential significance for informing hypotheses regarding seizure focus and guiding surgical interventions, particularly in patients with MRI-negative findings[15]. Prospective studies involving larger cohorts of epilepsy patients, consistent scan and sequence protocols, and advancements in post-processing technology are crucial for further exploration. Beyond technical enhancements, establishing a better correlation between imaging features and clinical semiology, histopathology, and overall clinical outcomes is equally important for the continued refinement of ultra-high-field MRI in epilepsy diagnosis and treatment[16].

Pituitary adenoma

When compared to standard-of-care clinical imaging at 3 T or 1.5 T, no significant difference in the visualization of pituitary adenoma features has been observed at 7 T. However, cranial nerves III, IV, and VI, ophthalmic arteries, and posterior communicating arteries were more effectively detected with 7T MRI than with lower field strength scans, and this superiority extended to comparisons with both 1.5 T and 3 T[17]. Furthermore, employing a granular, voxel-based analysis has been shown to maximize the potential of 7T imaging resolution and along with high-resolution apparent diffusion coefficient maps in 7T diffusion-weighted imaging (DWI), it represents a sensitive measure of pituitary adenoma consistency contributing to a more accurate characterization of their internal composition, providing valuable information for preoperative planning and predicting surgical outcomes[18,19]. In addition, 7T DWI has been succe-

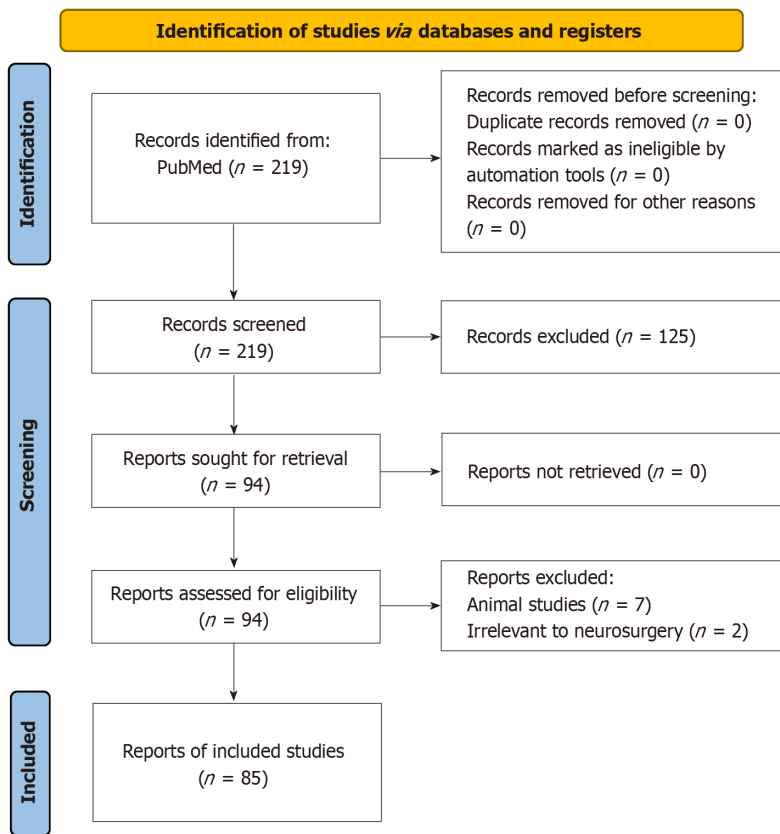


Figure 1 PRISMA flowchart depicting selection of studies for our systematic review.

successfully applied for probabilistic tractography of the optic tracts and radiations in patients with pituitary macroadenomas. The correlation between imaging findings and neuro-ophthalmological results offers an objective evaluation of damage to the anterior and posterior visual pathways, enhancing our ability to assess the impact of pituitary adenomas on visual function[20]. Quantifying secondary neuronal damage from adenomas through diffusion characteristics seen in 7T DWI enables preoperative characterization of visual pathway damage and facilitates prediction regarding recoverability of vision for patients experiencing chiasmatic compression[20,21]. The initial experience with ultra-high-field 7T MRI in patients with suspected Cushing’s disease and negative or equivocal imaging at conventional field strengths represents a critical aspect in detecting subtle abnormalities and may offer a valuable diagnostic tool in cases where conventional imaging falls short, contributing to improved diagnostic accuracy and patient management[22]. A recent study showed that 7T MRI facilitated the identification of previously unnoticed focal pituitary hypoenhancement in 90% (9/10) of patients. Remarkably, 7 out of these 9 cases corresponded histologically to corticotroph adenomas, indicating a significant adjunctive role for ultra-high-field MRI in the non-invasive clinical assessment of suspected Cushing's disease[22]. The use of 7T MRI proves valuable in identifying markers of endocrine function in patients with pituitary adenomas. The corrected T2 signal intensity (SI) of the tumor emerges as a sensitive predictor of hormonal secretion, offering utility in the diagnostic workup for pituitary adenoma. A study showed that hormone-secreting tumors exhibit higher T2-weighted SI and tumors associated with preoperative hypopituitarism display greater stalk curvature angles[23,24].

Parkinson's disease

Recently, Oh *et al*[25] employed high-resolution T1-weighted 7T MRI to investigate gray matter changes in Parkinson's disease (PD). The examination involved 12 patients and age- and sex-matched controls, with subgroup analysis based on the presence of axial motor symptoms. Utilizing an automated segmentation method, the study revealed distinctive patterns in cortical and subcortical volume alterations. PD patients exhibited global cortical atrophy, notably in the prefrontal area, including the rostral middle frontal, superior frontal, inferior parietal lobule, medial orbitofrontal, and rostral anterior cingulate regions while subcortical volume atrophy was observed in limbic/paralimbic areas such as the fusiform, hippocampus, and amygdala[25]. A recent study delved into the *in vivo* measurement of hippocampal subfields using ultra-high-field 7T MRI to understand whether these measures predict episodic memory impairment in PD. The findings provided insights into how structural changes within the hippocampus, such as the thickness of hippocampal CA1-SP subfield estimated by 7T MRI, could offer potential markers for early diagnosis and intervention of episodic memory impairment[26]. In the realm of advanced PD treatment, DBS targeting the subthalamic nucleus (STN) has proven highly effective. By assisting with target selection, 7T MRI has been shown to be capable of providing a more detailed and accurate representation of the brain anatomy, potentially improving the precision and efficacy of DBS procedures in PD patients[27]. Isaacs *et al*[28] conducted a study where three DBS-experienced neurosurgeons assessed optimal STN DBS target sites in three repetitions of 3T-T2, 7T-T2*, 7T-R2*, and 7T quantitative susceptibility mapping

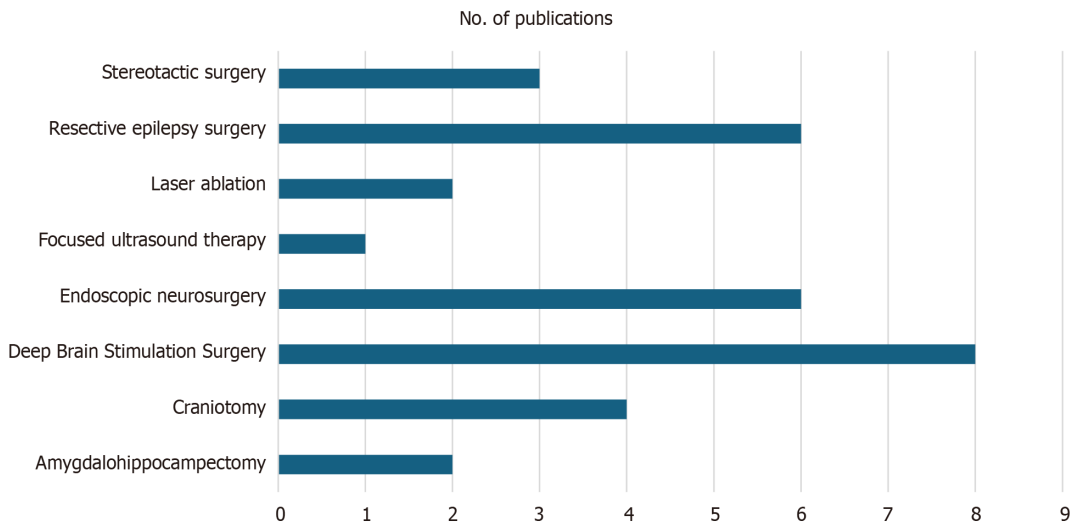


Figure 2 Chart showing number of 7T publications per neurosurgical procedure.

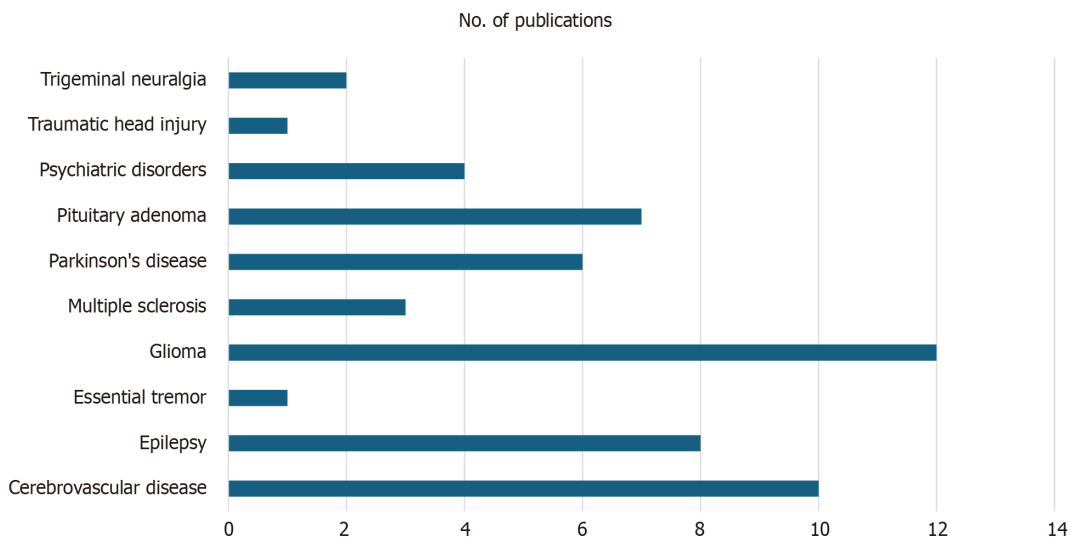


Figure 3 Chart showing number of 7T publications per neurosurgically treated pathology.

(QSM) images for five PD patients. The analysis showed that neurosurgeons were consistent in selecting the DBS target site across MRI field strengths, MRI contrast, and repetitions. However, when examining the coordinates in MNI space, it was observed that the chosen electrode location appeared to be more ventral with the 3T scan compared to the 7T scans. This suggests that while neurosurgeons maintain stability in their target selection, the higher anatomical information provided by 7T imaging might influence the actual location of the electrode during DBS placement[28]. A recent work outlined a workflow for integrating high-resolution *in vivo* ultra-high-field templates into the surgical navigation system to aid in DBS planning. Importantly, this method does not impose any additional cost or time on the patient. Future efforts will focus on prospectively evaluating various templates and assessing their impact on target selection[27]. A recent study based on 25 patients delved into the potential optimization of DBS through the combination of 7T T2-weighted and DWI sequences, enabling the selective segmentation of motor, associative, and limbic segments within the STN[17]. While the dorsolateral STN consistently housed the highest density of motor connections, the specific partitioning of segments varied among patients[29]. Notably, active electrode contacts within the predominantly motor-connected segment exhibited an average hemi-body unified PD rating scale motor improvement of 80%, contrasting with 52% outside this segment ($P < 0.01$). The study concluded that implementing 7T T2 and DWI segmentation offers insights into the location of the motor segment in DBS for PD[29]. Guided electrode placement based on segmentation is anticipated to enhance motor response, yet widespread implementation would benefit from the availability of commercial DBS software for postprocessing imaging[29]. In addition, a recent study aimed to validate the clinical application accuracy of the 7T-machine learning (ML) method by comparing it with the identification of the STN based on intraoperative microelectrode recordings and demonstrated that the 7T-ML method demonstrates high consistency with microelectrode-recordings data, offering a reliable and accurate patient-specific prediction for targeting the STN[30].

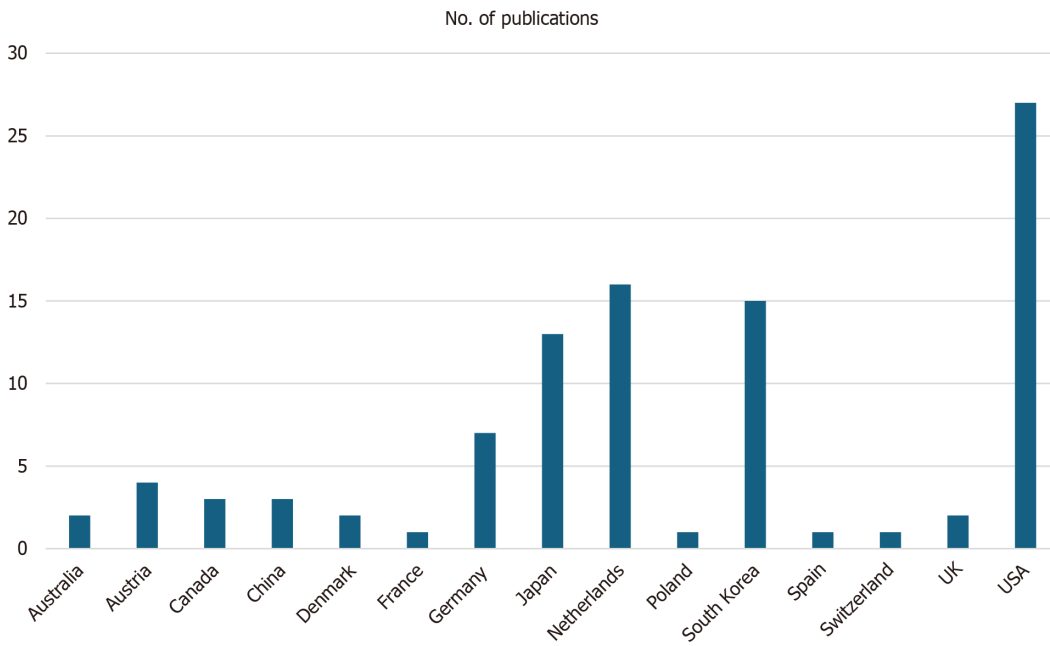


Figure 4 Histogram showing number of 7T publications per country.

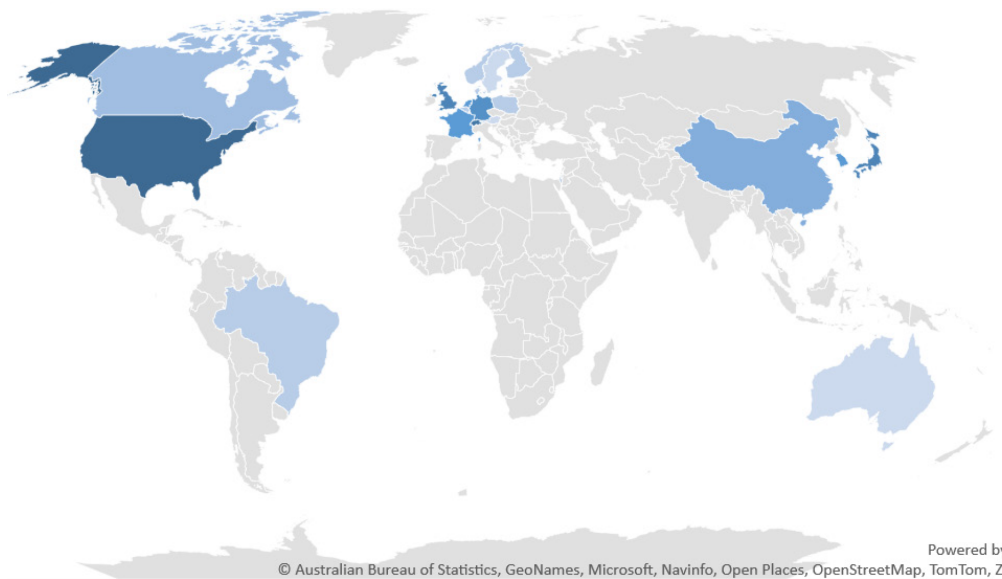


Figure 5 7-Tesla magnetic resonance imaging facilities per country. Australia (2), Austria (2), Belgium (1), Brazil (1), Canada (3), China (9), Denmark (1), Finland (1), France (4), Germany (18), Israel (1), Japan (6), Netherlands (4), Norway (1), Poland (1), South Korea (4), Sweden (2), Switzerland (5), United Kingdom (6), United States (35).

Cerebrovascular diseases

Comparison of 3T and 7T MRI in visualizing intracranial arterial vessel wall and vessel wall lesions has demonstrated the potential superiority of 7T MRI in providing enhanced resolution and detailed characterization of vessel wall abnormalities in cerebrovascular diseases[31]. Despite considerable variability in detected lesions at both field strengths, 7T MRI has the highest potential for identifying the overall burden of intracranial vessel wall lesions[31]. For example, a prospective evaluation of the utility of non-contrast-enhanced 7T magnetic resonance (MR) angiography (MRA) for delineating UIAs within a clinical setting showed comparability to the gold standard, digital subtraction angiography. The combined use of 7T non-enhanced magnetization-prepared rapid gradient echo and time-of-flight MRA for evaluating untreated UIAs emerges as a promising clinical application of ultra-high-field MRA[32]. Delineation of regions of wall weak in intracranial aneurysms has been performed using 7T MRI to identify areas prone to rupture, providing valuable insights into the structural characteristics of aneurysm walls and potentially contributing to risk stratification and personalized treatment strategies[33]. In most cases, there was an observed hyperintense rim effect along the vessel wall where there were demonstrated elevated values of mean wall shear stress (WSS) and vorticity, as analyzed by computational fluid dynamics[33]. In a retrospective, cross-sectional study utilizing 4D flow MRI at 7 T, the hemo-

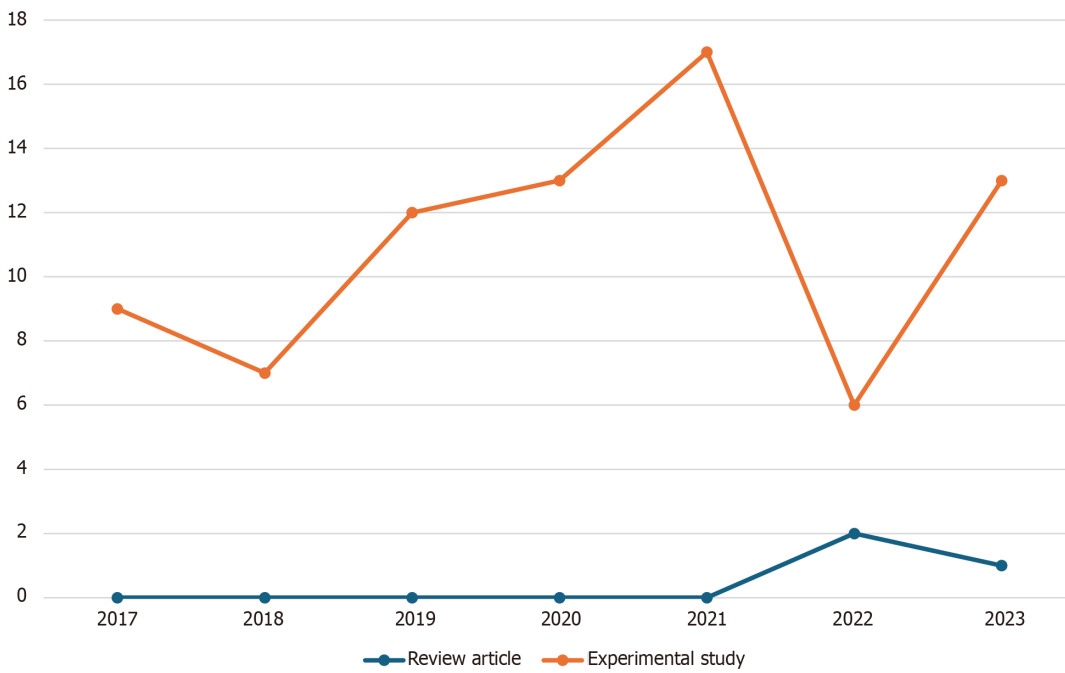


Figure 6 Illustration of number of 7T publications, both review papers and experimental studies, published in each year from 2017 to 2023.

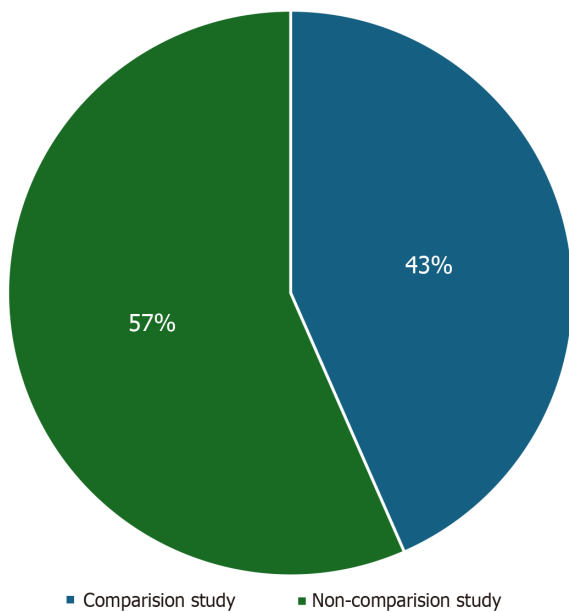


Figure 7 Pie chart showing share of comparison vs non-comparison studies.

dynamic characteristics along the circle of Willis have been investigated to gain insights into the development of UIAs [34]. Thirty-eight patients with UIAs, primarily women with a mean age of 62 years, were assessed for hemodynamic parameters in the parent artery of the UIA compared to the corresponding contralateral artery without a UIA. Results indicated significant differences in blood flow, mean velocity, WSS maxima and mean values, and velocity pulsatility index between the two arteries. Importantly, WSSmax increases linearly, while WSSmean decreases linearly with increasing UIA size. The findings suggested distinct hemodynamic variations between vessels with and without UIAs and highlighted the potential role of WSS in the pathology of aneurysm development[34]. The radiofrequency (RF)-induced tissue heating around aneurysm clips during a 7T head MR examination was also evaluated and aimed to determine the decoupling distance between multiple implanted clips to ensure the safety and feasibility of 7T MRI in these patients[35]. In a 7T ultra-high field MRI setting, safe scanning conditions regarding RF-induced heating can be implemented for single or decoupled aneurysm clips; however, more research is required for cases involving multiple aneurysm clips separated by less than 35 mm to ensure safety in this specific configuration[35]. The potential of oxygen

extraction fraction (OEF) maps generated by MR QSM at 7 T in detecting OEF changes was also investigated. The comparison with positron emission tomography (PET) results establishes the capability of 7T MRI to non-invasively monitor OEF alterations, offering a valuable alternative to traditional imaging modalities, ultimately helping avoid unnecessary radiation exposure[36]. In patients with unilateral steno-occlusive internal carotid artery/middle cerebral artery lesions, OEF ratios on 7T QSM images demonstrated a strong correlation with those on PET images, suggesting that OEF measurement by MRI has the potential to serve as a substitute for PET[36]. A study also explored the use of whole-brain MRA at 7 T for the non-invasive detection of impaired cerebrovascular reactivity in patients in an attempt to assess cerebrovascular function in patients with chronic cerebral ischemia[37]. The occurrence of a striped occipital cortex and intragyral hemorrhage, previously detected on ultra-high-field 7T MRI in hereditary cerebral amyloid angiopathy (CAA), was recently investigated. Researchers aimed to determine whether these markers are also present in sporadic CAA (sCAA) or non-sCAA ICH, contributing to the understanding of imaging markers in different forms of CAA[38]. While a striped occipital cortex was uncommon in superficial cortical siderosis (sCAA), approximately 12% of patients with sCAA exhibited intragyral hemorrhages which were also found to be associated with advanced disease, and their absence in patients with non-superficial cortical siderosis ICHs may suggest a level of specificity for CAA[38]. The presence and extent of contrast agent leakage distant from the hematoma were found as a marker of blood-brain barrier (BBB) disruption in patients with spontaneous ICH occurring in the previous days or weeks. The use of 7T MRI allows for a detailed examination of BBB integrity, providing valuable information on the extent of vascular damage in the surrounding brain tissue[39]. Next, a study compared cerebral cavernous malformations (CCMs)-associated cerebral venous angioarchitecture between sporadic and familial cases using 7T MRI. This investigation provided insights into the vascular alterations associated with CCMs, potentially aiding in the differentiation and characterization of familial and sporadic cases[40]. The susceptibility-weighted imaging (SWI) results of the venous angioarchitecture of multiple CCMs were consistent with the theory that venous anomalies are causative for the sporadic form of multiple CCMs[40].

Trigeminal neuralgia

7T MRI has been explored for investigating diffusion tensor imaging (DTI) parameters and assessing the feasibility of DTI criteria for diagnosing trigeminal neuralgia (TN). By examining the microstructural integrity of the trigeminal nerve, researchers aimed to identify specific DTI parameters that may serve as diagnostic indicators for TN[41]. 7T MRI was employed to investigate the central causal mechanisms of TN and the surrounding brain structure. By comparing healthy controls (HCs) with patients suffering from TN, researchers aimed to identify structural and functional alterations in the trigeminal nerve and associated brain regions. The high resolution and sensitivity of 7T MRI enable a detailed examination, shedding light on potential biomarkers and contributing to our understanding of the underlying mechanisms of TN[42]. Results suggest that the central anterior cingulate cortex and posterior cingulate cortex, but not the rostral anterior cingulate cortex, are associated with central pain mechanisms in TN[42].

Traumatic head injury

A study examined the potential prognostic advantages of utilizing 7T SWI for traumatic cerebral microbleeds (TMBs) in comparison to 3T SWI. The aim was to forecast the immediate clinical condition and subjective impairments, encompassing health-related quality of life, following a closed head injury (CHI). The number of TMBs showed a substantial association with indicators of the acute clinical state and chronic neurobehavioral parameters after a CHI, but there was no additional advantage of 7T MRI. These preliminary findings warrant a larger prospective study for the future[43].

Multiple sclerosis

Fluid-attenuated inversion recovery (FLAIR) imaging at 3 T is recognized as the most sensitive method for identifying white matter lesions in multiple sclerosis (MS). Although 7T FLAIR effectively detects cortical lesions, it has not been fully optimized for visualizing white matter lesions, thus limiting its use in delineating lesions in quantitative MRI studies of normal-appearing white matter in MS. As a result, a team assessed the sensitivity of 7T magnetization-transfer-weighted (MTw) images in detecting white matter lesions in comparison to 3T FLAIR. The findings indicate that 7T MTw sequences successfully identified the majority of white matter lesions detected by FLAIR at 3 T, thus implying that 7T MTw imaging can serve as a robust alternative alongside 3T FLAIR. Subsequent studies should explore and compare the roles of optimized 7T-FLAIR and 7T-MTw imaging[44]. A recent study aimed to pinpoint white matter tracts (WMTs) associated with the severity of neurogenic lower urinary tract dysfunction (NLUTD) in women with MS[45]. The primary cohort included 28 women with MS and NLUTD, and a validation cohort comprised 10 women with similar conditions. Both cohorts underwent clinical assessments and functional MRI protocols, with the validation cohort additionally undergoing a 7T fMRI scan[45]. The study identified a robust correlation between fractional anisotropy and mean diffusivity of specific WMTs and clinical parameters related to NLUTD symptoms in women with MS, notably the right inferior cerebellar peduncle, left posterior limb of the internal capsule, and left superior cerebellar peduncle[45]. Another study aimed to characterize cortical lesions in MS using 7T T2/T1-weighted MRI and assess their relationship with other MS pathology and impact on disability[46]. In 64 adults with MS (45 relapsing-remitting/19 progressive), cortical lesions were identified in 94%, with a higher burden in progressive MS compared to relapsing-remitting MS. The distribution of lesions across 50 cortical regions was nonuniform, with the highest lesion burden in the supplementary motor cortex and the highest prevalence in the superior frontal gyrus. Leukocortical lesions were strongly correlated with white matter lesions and paramagnetic rim lesions, while subpial lesions showed a moderate correlation; however, both were correlated with spinal cord lesions. Cortical lesion volumes, including subtypes, were correlated with disability measures, suggesting their significant role in the clinical course of MS[46].

Glioma

Ultra-high-field MRI of the brain is an appealing option for image guidance during neurosurgery due to its superior tissue contrast and detailed vessel visualization. However, the susceptibility of high-field MRI to distortion artifacts poses a potential challenge to image guidance accuracy. In a study, researchers specifically examined intra- and extracranial distortions in 7T MRI scans. Upon inspection of magnetization-prepared T1-weighted 7T MRI cranial images, no discernible intracranial distortions were observed. However, noteworthy extracranial shifts were identified, introducing a level of unreliability in 7T images when used for patient-to-image registration. To address this issue, researchers recommend conducting patient-to-image registration on a standard imaging modality, such as a routine computed tomography scan or a 3T MR image. Subsequently, the 7T MRI image can be fused with the routine image on the image guidance machine. This proposed approach is advised until a resolution is achieved for the observed extracranial shifts in 7T MRI scans[47]. An exploratory study aimed to assess the potential clinical implications of single-voxel 7T MR spectroscopy (MRS) in patients with grades II and III gliomas[48]. Seven patients and seven HCs were scanned, and metabolic ratios were calculated relative to water and total creatine. The results revealed significant increases in choline/creatinine and myoinositol/creatinine ratios, along with decreases in N-acetyl aspartate/creatinine and glutamate/creatinine ratios when comparing tumor data to control regions[48]. The N-acetyl aspartate/water and glutamate/water ratios also showed significant decreases. Lactate/water and lactate/creatinine ratios displayed increases, albeit not significant. GABA/water ratio was significantly decreased, and MRS spectra confirmed the presence of 2-hydroxyglutarate in three out of four patients studied. Overall, the study, conducted at 7 T, yielded results consistent with existing literature on both 3T and 7T MRS in glioma research[48]. In a retrospective study of 84 glioma patients, the potential for preoperative identification of isocitrate dehydrogenase (IDH) mutation status in glioma was explored using a combination of convolutional neural network (CNN) and ultra-high-field 7T chemical exchange saturation transfer (CEST) imaging[49]. The study demonstrated the potential of ultra-high-field CEST and CNN for improving sensitivity and specificity in predicting IDH mutation status, surpassing radionics-based predictions in various metrics. The authors emphasized the promising role of this approach in clinical decision-making while acknowledging the need for further improvement in accuracy through expanded datasets and addressing B1 inhomogeneities[49]. Using high fluoro-ethyl-L-tyrosine uptake as the standard, the combination of CEST and MRS was shown to outperform individual modalities in predicting tumor infiltration, presenting a promising alternative for delineating glioma extent without the use of radioactive tracers. The study's preliminary verification through multi-region biopsies supports the potential clinical relevance of the 7T CEST/MRS combination in guiding tumor resection and irradiation[50].

Psychiatric disorders

A team explored the potential for individuals to acquire the skill of dynamically controlling the activity of the dorsolateral prefrontal cortex (DLPFC). The DLPFC is recognized for its significance in working memory function and its association with various psychiatric disorders. This study also sought to delve into the learnability of such dynamic control, which may have implications for our understanding of cognitive processes and mental health conditions[51]. These findings offer an initial indication that individuals may have the capacity to learn to dynamically down-regulate physiological activity in the DLPFC. This has potential implications for psychiatric disorders in which the DLPFC plays a significant role[51]. Another study utilized a combination of high-resolution and quantitative MRI, employing both supervised and unsupervised computational techniques. This approach enabled the acquisition of robust sub-millimeter measurements of the locus coeruleus (LC) *in vivo*. Additionally, the study investigated the correlation of these measurements with prevalent psychopathological conditions. The implications of this work extend broadly, as it holds the potential to impact various neurological and psychiatric disorders known for their association with anticipated LC dysfunction[52]. This study combined high-resolution and quantitative MR with a mixture of supervised and unsupervised computational techniques to provide robust, sub-millimeter measurements of the LC *in vivo*, which were additionally related to common psychopathology. This work has wide-reaching applications for a range of neurological and psychiatric disorders characterized by expected LC dysfunction[52]. In a recent study, 22 PD patients who underwent STN DBS were categorized into apathy and non-apathy groups based on changes in the Starkstein Apathy Scale score 6 mo post-DBS[53]. Using 7T MRI subthalamic network analysis, the location of active DBS contacts relative to STN subdivisions (motor, associative, and limbic) was visualized. The analysis revealed that active contacts in apathy patients were more often positioned within or close to the area within the STN with a high density of surrounding projections to associative cortex areas compared to non-apathy patients (63% vs 42%, $P = 0.02$). Conversely, the density of surrounding motor projections was lower in the apathy group (18%) than in the non-apathy group (38%, $P = 0.01$). The study suggests an anatomical connectivity substrate for apathy in DBS, emphasizing the importance of considering the location of active contacts within the STN in relation to its subdivisions for understanding and potentially mitigating apathy in PD patients undergoing DBS[53]. A study aimed to explore volumetric differences in hippocampal subfields between patients with major depressive disorder (MDD), specifically treatment-resistant depression (TRD), and HCs using automatic segmentation of hippocampal subfields software with ultra-high-field 7T MRI[54]. The results revealed reduced right-hemisphere CA2/3 subfield volume in both MDD and TRD patients compared to HCs. Moreover, negative associations were found between subfield volumes and life-stressor checklist scores. The study highlights the potential of high-resolution MRI data and automated segmentation techniques to identify biomarkers for MDD and TRD, providing insights into the pathophysiology of depression and potential implications for treatment selection. However, the authors acknowledge the need for caution in interpreting these results due to the small sample size and low power, emphasizing the importance of further research in this area[54].

Limitations of our analysis

It is essential to highlight the limitations of our study. Initially, it is worth noting that our examination of records might have overlooked certain publications cataloged in alternative databases such as EMBASE, Scopus, Google Scholar, among others. Nevertheless, PubMed is renowned for its accurate and top-tier content sourced from peer-reviewed medical journals, underscoring its suitability for conducting systematic reviews in the medical field. Systematic reviews inherently involve a balance between comprehensiveness and practicality, and the inclusion of an excessive number of databases can lead to cumbersome processing times. In addition, we would like to highlight that a manual exploration of EMBASE using identical search criteria revealed minimal oversight of studies, indicating that the decision to abstain from its utilization incurred relatively minor drawbacks. Study selection bias could have occurred due to restriction to English language records, and search strategy constraints such as the non-inclusion of terms such as 7 T and 7-T potentially leading to skewed conclusions by systematically excluding certain studies. Excluding grey literature further compounds this issue, as valuable data from unpublished sources may be overlooked, resulting in an incomplete representation of evidence. Publication bias exacerbates these concerns, favoring the publication of studies with positive or significant results and potentially distorting the overall evidence base. Another limitation of our study was that if an author affiliated to the Neurosurgery Department was involved in the manuscript, the study was included even though a neurosurgical procedure was not discussed in the article. Lastly, although we retrieved a total of 85 studies into our database, only 49 out of those have been referenced in this review in [Table 1](#) since their findings were relevant to a specific pathology while the remaining have only been denoted in the figures (were used only for analysis and generation of the data)[55-57].

CONCLUSION

The findings open avenues for further exploration and integration of 7T imaging into routine clinical practice, promising improved patient outcomes and refined surgical interventions. However, this will be possible only if the distribution of 7T MR systems is accelerated worldwide and radiologists receive enough training regarding safety measures, feasibility, and other challenges. The adoption of 7T MRI faces significant barriers, primarily revolving around its substantial cost and potential side effects. With the machine alone costing approximately 6.5 million dollars, considerations extend to the energy consumption and space requirements. Moreover, concerns regarding side effects such as vertigo further impede its acceptance. Safety issues arise due to the stronger magnetic field, posing risks to patients with metallic implants or devices, alongside challenges in achieving consistent image quality and contrast uniformity. Regulatory hurdles for clinical application also loom large. To surmount these obstacles, concerted efforts are essential. Ongoing research is crucial to address safety concerns and establish clear guidelines for safe usage. Advancements in imaging techniques and software are necessary to enhance image quality. Collaborative endeavors among researchers, clinicians, and regulators are pivotal for setting standards and protocols, defining gold standards for clinical use. Additionally, increasing awareness and providing education on the manifold benefits of 7T MRI are imperative to foster its wider adoption in clinical practice. A continuously updated list of 7T MRI facilities and their relevant locations globally can be accessed at <https://www.google.com/maps/d/u/0/viewer?ll=1.941826124046989%2C0&z=2&mid=1dXG84OZIAOxjsq-h3x2tGzWL1bNU>.

FOOTNOTES

Author contributions: Perera Molligoda Arachchige AS conceived of the presented idea and performed the analysis; Catapano F and Politi LS verified the analytical methods. All authors discussed the results and contributed to writing the final manuscript.

Conflict-of-interest statement: The authors have no conflicts of interest to declare.

PRISMA 2009 Checklist statement: The authors have read the PRISMA 2009 Checklist, and the manuscript was prepared and revised according to the PRISMA 2009 Checklist.

Open-Access: This article is an open-access article that was selected by an in-house editor and fully peer-reviewed by external reviewers. It is distributed in accordance with the Creative Commons Attribution NonCommercial (CC BY-NC 4.0) license, which permits others to distribute, remix, adapt, build upon this work non-commercially, and license their derivative works on different terms, provided the original work is properly cited and the use is non-commercial. See: <https://creativecommons.org/licenses/by-nc/4.0/>

Country of origin: Italy

ORCID number: Arosh S Perera Molligoda Arachchige 0000-0002-3875-0267; Letterio S Politi 0000-0002-6190-6688.

S-Editor: Qu XL

L-Editor: Wang TQ

P-Editor: Che XX

REFERENCES

- 1 Arachchige ASPM. Transitioning from PET/MR to trimodal neuroimaging: why not cover the temporal dimension with EEG? *AIMS Neurosci* 2023; **10**: 1-4 [PMID: 37077957 DOI: 10.3934/Neuroscience.2023001]
- 2 Perera Molligoda Arachchige AS. Neuroimaging with PET/MR: moving beyond 3 T in preclinical systems, when for clinical practice? *Clin Transl Imaging* 2023; **11**: 315-319 [DOI: 10.1007/s40336-023-00572-6]
- 3 Arachchige ASPM. 7-Tesla PET/MRI: A promising tool for multimodal brain imaging? *AIMS Neurosci* 2022; **9**: 516-518 [PMID: 36660074 DOI: 10.3934/Neuroscience.2022029]
- 4 Verma Y, Ramesh S, Perera Molligoda Arachchige AS. 7 T Versus 3 T in the Diagnosis of Small Unruptured Intracranial Aneurysms: Reply to Radojewski et al. *Clin Neuroradiol* 2024; **34**: 51-52 [PMID: 37318559 DOI: 10.1007/s00062-023-01321-y]
- 5 Cosottini M, Roccatagliata L. Neuroimaging at 7 T: are we ready for clinical transition? *Eur Radiol Exp* 2021; **5**: 37 [PMID: 34435257 DOI: 10.1186/s41747-021-00234-0]
- 6 Okada T, Fujimoto K, Fushimi Y, Akasaka T, Thuy DHD, Shima A, Sawamoto N, Oishi N, Zhang Z, Funaki T, Nakamoto Y, Murai T, Miyamoto S, Takahashi R, Isa T. Neuroimaging at 7 Tesla: a pictorial narrative review. *Quant Imaging Med Surg* 2022; **12**: 3406-3435 [PMID: 35655840 DOI: 10.21037/qims-21-969]
- 7 Whiting PF, Rutjes AW, Westwood ME, Mallett S, Deeks JJ, Reitsma JB, Leeflang MM, Sterne JA, Bossuyt PM; QUADAS-2 Group. QUADAS-2: a revised tool for the quality assessment of diagnostic accuracy studies. *Ann Intern Med* 2011; **155**: 529-536 [PMID: 22007046 DOI: 10.7326/0003-4819-155-8-201110180-00009]
- 8 Sterne JAC, Savović J, Page MJ, Elbers RG, Blencowe NS, Boutron I, Cates CJ, Cheng HY, Corbett MS, Eldridge SM, Emberson JR, Hernán MA, Hopewell S, Hróbjartsson A, Junqueira DR, Jüni P, Kirkham JJ, Lasserson T, Li T, McAleenan A, Reeves BC, Shepperd S, Shrier I, Stewart LA, Tilling K, White IR, Whiting PF, Higgins JPT. RoB 2: a revised tool for assessing risk of bias in randomised trials. *BMJ* 2019; **366**: l4898 [PMID: 31462531 DOI: 10.1136/bmj.l4898]
- 9 Page MJ, McKenzie JE, Bossuyt PM, Boutron I, Hoffmann TC, Mulrow CD, Shamseer L, Tetzlaff JM, Akl EA, Brennan SE, Chou R, Ghanville J, Grimshaw JM, Hróbjartsson A, Lalu MM, Li T, Loder EW, Mayo-Wilson E, McDonald S, McGuinness LA, Stewart LA, Thomas J, Tricco AC, Welch VA, Whiting P, Moher D. The PRISMA 2020 statement: an updated guideline for reporting systematic reviews. *BMJ* 2021; **372**: n71 [PMID: 33782057 DOI: 10.1136/bmj.n71]
- 10 Stefanits H, Springer E, Pataria E, Baumgartner C, Hainfellner JA, Prayer D, Weisstanner C, Czech T, Trattinig S. Seven-Tesla MRI of Hippocampal Sclerosis: An In Vivo Feasibility Study With Histological Correlations. *Invest Radiol* 2017; **52**: 666-671 [PMID: 28538339 DOI: 10.1097/RLI.0000000000000388]
- 11 Zhang Y, Lv Y, You H, Dou W, Hou B, Shi L, Zuo Z, Mao W, Feng F. Study of the hippocampal internal architecture in temporal lobe epilepsy using 7 T and 3 T MRI. *Seizure* 2019; **71**: 116-123 [PMID: 31325818 DOI: 10.1016/j.seizure.2019.06.023]
- 12 Wang I, Oh S, Blümcke J, Coras R, Krishnan B, Kim S, McBride A, Grinenko O, Lin Y, Overmyer M, Aung TT, Lowe M, Larvie M, Alexopoulos AV, Bingaman W, Gonzalez-Martinez JA, Najm I, Jones SE. Value of 7T MRI and post-processing in patients with nonlesional 3T MRI undergoing epilepsy presurgical evaluation. *Epilepsia* 2020; **61**: 2509-2520 [PMID: 32949471 DOI: 10.1111/epi.16682]
- 13 Veersema TJ, Ferrier CH, van Eijsden P, Gosselaar PH, Aronica E, Visser F, Zwanenburg JM, de Kort GAP, Hendrikse J, Luijten PR, Braun KPJ. Seven tesla MRI improves detection of focal cortical dysplasia in patients with refractory focal epilepsy. *Epilepsia Open* 2017; **2**: 162-171 [PMID: 29588945 DOI: 10.1002/epi4.12041]
- 14 Sharma HK, Feldman R, Delman B, Rutland J, Marcuse LV, Fields MC, Ghatan S, Panov F, Singh A, Balchandani P. Utility of 7 tesla MRI brain in 16 "MRI Negative" epilepsy patients and their surgical outcomes. *Epilepsy Behav Rep* 2021; **15**: 100424 [PMID: 33521618 DOI: 10.1016/j.ebr.2020.100424]
- 15 Rutland JW, Feldman RE, Delman BN, Panov F, Fields MC, Marcuse LV, Hof PR, Lin HM, Balchandani P. Subfield-specific tractography of the hippocampus in epilepsy patients at 7 Tesla. *Seizure* 2018; **62**: 3-10 [PMID: 30245458 DOI: 10.1016/j.seizure.2018.09.005]
- 16 van Lanen RHGJ, Colon AJ, Wiggins CJ, Hoebregts MC, Hoogland G, Roebroek A, Ivanov D, Poser BA, Rouhl RPW, Hofman PAM, Jansen JFA, Backes W, Rijkers K, Schijns OEMG. Ultra-high field magnetic resonance imaging in human epilepsy: A systematic review. *Neuroimage Clin* 2021; **30**: 102602 [PMID: 33652376 DOI: 10.1016/j.nicl.2021.102602]
- 17 Rutland JW, Delman BN, Feldman RE, Tsankova N, Lin HM, Padormo F, Shrivastava RK, Balchandani P. Utility of 7 Tesla MRI for Preoperative Planning of Endoscopic Endonasal Surgery for Pituitary Adenomas. *J Neurol Surg B Skull Base* 2021; **82**: 303-312 [PMID: 34026406 DOI: 10.1055/s-0039-3400222]
- 18 Yao A, Rutland JW, Verma G, Banihashemi A, Padormo F, Tsankova NM, Delman BN, Shrivastava RK, Balchandani P. Pituitary adenoma consistency: Direct correlation of ultrahigh field 7T MRI with histopathological analysis. *Eur J Radiol* 2020; **126**: 108931 [PMID: 32146344 DOI: 10.1016/j.ejrad.2020.108931]
- 19 Perera Molligoda Arachchige AS, Politi LS. Potential applications of 7 Tesla magnetic resonance imaging in paediatric neuroimaging: Feasibility and challenges. *World J Clin Pediatr* 2024; **13**: 90641 [DOI: 10.5409/wjcp.v13.i2.90641]
- 20 Rutland JW, Padormo F, Yim CK, Yao A, Arrighi-Allisan A, Huang KH, Lin HM, Chelnis J, Delman BN, Shrivastava RK, Balchandani P. Quantitative assessment of secondary white matter injury in the visual pathway by pituitary adenomas: a multimodal study at 7-Tesla MRI. *J Neurosurg* 2019; **132**: 333-342 [PMID: 30660127 DOI: 10.3171/2018.9.JNS182022]
- 21 Rutland JW, Delman BN, Huang KH, Verma G, Benson NC, Villavisanis DF, Lin HM, Bederson JB, Chelnis J, Shrivastava RK, Balchandani P. Primary visual cortical thickness in correlation with visual field defects in patients with pituitary macroadenomas: a structural 7-Tesla retinotopic analysis. *J Neurosurg* 2019; **133**: 1371-1381 [PMID: 31628280 DOI: 10.3171/2019.7.JNS191712]
- 22 Patel V, Liu CJ, Shiroishi MS, Hurth K, Carmichael JD, Zada G, Toga AW. Ultra-high field magnetic resonance imaging for localization of corticotropin-secreting pituitary adenomas. *Neuroradiology* 2020; **62**: 1051-1054 [PMID: 32306052 DOI: 10.1007/s00234-020-02431-x]
- 23 Rutland JW, Loewenstern J, Ranti D, Tsankova NM, Bellaire CP, Bederson JB, Delman BN, Shrivastava RK, Balchandani P. Analysis of 7-tesla diffusion-weighted imaging in the prediction of pituitary macroadenoma consistency. *J Neurosurg* 2020; **134**: 771-779 [PMID: 32109870 DOI: 10.3171/2019.12.JNS192940]
- 24 Rutland JW, Pawha P, Belani P, Delman BN, Gill CM, Brown T, Cheesman K, Shrivastava RK, Balchandani P. Tumor T2 signal intensity and stalk angulation correlates with endocrine status in pituitary adenoma patients: a quantitative 7 tesla MRI study. *Neuroradiology* 2020; **62**: 473-482 [PMID: 31925468 DOI: 10.1007/s00234-019-02352-4]
- 25 Oh BH, Moon HC, Kim A, Kim HJ, Cheong CJ, Park YS. Prefrontal and hippocampal atrophy using 7-tesla magnetic resonance imaging in

- patients with Parkinson's disease. *Acta Radiol Open* 2021; **10**: 2058460120988097 [PMID: 33786201 DOI: 10.1177/2058460120988097]
- 26 **La C**, Linortner P, Bernstein JD, Ua Cruadhlaioich MAI, Fenesy M, Deutsch GK, Rutt BK, Tian L, Wagner AD, Zeineh M, Kerchner GA, Poston KL. Hippocampal CA1 subfield predicts episodic memory impairment in Parkinson's disease. *Neuroimage Clin* 2019; **23**: 101824 [PMID: 31054380 DOI: 10.1016/j.nicl.2019.101824]
- 27 **Lau JC**, MacDougall KW, Arango MF, Peters TM, Parrent AG, Khan AR. Ultra-High Field Template-Assisted Target Selection for Deep Brain Stimulation Surgery. *World Neurosurg* 2017; **103**: 531-537 [PMID: 28427973 DOI: 10.1016/j.wneu.2017.04.043]
- 28 **Isaacs BR**, Heijmans M, Kuijf ML, Kubben PL, Ackermans L, Temel Y, Keuken MC, Forstmann BU. Variability in subthalamic nucleus targeting for deep brain stimulation with 3 and 7 Tesla magnetic resonance imaging. *Neuroimage Clin* 2021; **32**: 102829 [PMID: 34560531 DOI: 10.1016/j.nicl.2021.102829]
- 29 **Mathiopoulou V**, Rijks N, Caan MWA, Liebrand LC, Ferreira F, de Bie RMA, van den Munckhof P, Schuurman PR, Bot M. Utilizing 7-Tesla Subthalamic Nucleus Connectivity in Deep Brain Stimulation for Parkinson Disease. *Neuromodulation* 2023; **26**: 333-339 [PMID: 35216874 DOI: 10.1016/j.neurom.2022.01.003]
- 30 **Shamir RR**, Duchin Y, Kim J, Patriat R, Marmor O, Bergman H, Vitek JL, Sapiro G, Bick A, Eliahou R, Eitan R, Israel Z, Harel N. Microelectrode Recordings Validate the Clinical Visualization of Subthalamic-Nucleus Based on 7T Magnetic Resonance Imaging and Machine Learning for Deep Brain Stimulation Surgery. *Neurosurgery* 2019; **84**: 749-757 [PMID: 29800386 DOI: 10.1093/neuros/nyy212]
- 31 **Harteveld AA**, van der Kolk AG, van der Worp HB, Dieleman N, Siero JCW, Kuijf HJ, Frijns CJM, Luijten PR, Zwanenburg JJM, Hendrikse J. High-resolution intracranial vessel wall MRI in an elderly asymptomatic population: comparison of 3T and 7T. *Eur Radiol* 2017; **27**: 1585-1595 [PMID: 27387876 DOI: 10.1007/s00330-016-4483-3]
- 32 **Wrede KH**, Matsushige T, Goericke SL, Chen B, Umütlu L, Quick HH, Ladd ME, Johst S, Forsting M, Sure U, Schlamann M. Non-enhanced magnetic resonance imaging of unruptured intracranial aneurysms at 7 Tesla: Comparison with digital subtraction angiography. *Eur Radiol* 2017; **27**: 354-364 [PMID: 26993650 DOI: 10.1007/s00330-016-4323-5]
- 33 **Millesi M**, Knosp E, Mach G, Hainfellner JA, Ricken G, Trattinig S, Gruber A. Focal irregularities in 7-Tesla MRI of unruptured intracranial aneurysms as an indicator for areas of altered blood-flow parameters. *Neurosurg Focus* 2019; **47**: E7 [PMID: 31786557 DOI: 10.3171/2019.9.FOCUS19489]
- 34 **van Tuijl RJ**, Timmins KM, Velthuis BK, van Ooij P, Zwanenburg JJM, Ruigrok YM, van der Schaaf IC. Hemodynamic Parameters in the Parent Arteries of Unruptured Intracranial Aneurysms Depend on Aneurysm Size and Are Different Compared to Contralateral Arteries: A 7 Tesla 4D Flow MRI Study. *J Magn Reson Imaging* 2024; **59**: 223-230 [PMID: 37144669 DOI: 10.1002/jmri.28756]
- 35 **Noureddine Y**, Kraff O, Ladd ME, Wrede K, Chen B, Quick HH, Schaefer G, Bitz AK. Radiofrequency induced heating around aneurysm clips using a generic birdcage head coil at 7 Tesla under consideration of the minimum distance to decouple multiple aneurysm clips. *Magn Reson Med* 2019; **82**: 1859-1875 [PMID: 31199013 DOI: 10.1002/mrm.27835]
- 36 **Uwano I**, Kudo K, Sato R, Ogasawara K, Kameda H, Nomura JI, Mori F, Yamashita F, Ito K, Yoshioka K, Sasaki M. Noninvasive Assessment of Oxygen Extraction Fraction in Chronic Ischemia Using Quantitative Susceptibility Mapping at 7 Tesla. *Stroke* 2017; **48**: 2136-2141 [PMID: 28663515 DOI: 10.1161/STROKEAHA.117.017166]
- 37 **Uwano I**, Kameda H, Harada T, Kobayashi M, Yanagihara W, Setta K, Ogasawara K, Yoshioka K, Yamashita F, Mori F, Matsuda T, Sasaki M. Detection of impaired cerebrovascular reactivity in patients with chronic cerebral ischemia using whole-brain 7T MRA. *J Stroke Cerebrovasc Dis* 2020; **29**: 105081 [PMID: 32807478 DOI: 10.1016/j.jstrokecerebrovasdis.2020.105081]
- 38 **Koemans EA**, Voigt S, Rasing I, Jolink W, van Harten TW, van der Grond J, van Rooden S, Schreuder F, Freeze WM, van Buchem MA, van Zwet EW, van Veluw SJ, Terwindt GM, van Osch M, Klijn C, van Walderveen M, Wermer M. Striped occipital cortex and intragray hemorrhage: Novel magnetic resonance imaging markers for cerebral amyloid angiopathy. *Int J Stroke* 2021; **16**: 1031-1038 [PMID: 33535905 DOI: 10.1177/1747493021991961]
- 39 **Jolink WM**, Lindenholtz A, van Etten ES, van Nieuwenhuizen KM, Schreuder FH, Kuijf HJ, van Osch MJ, Hendrikse J, Rinkel GJ, Wermer MJ, Klijn CJ. Contrast leakage distant from the hematoma in patients with spontaneous ICH: A 7 T MRI study. *J Cereb Blood Flow Metab* 2020; **40**: 1002-1011 [PMID: 31142225 DOI: 10.1177/0271678X19852876]
- 40 **Dammann P**, Wrede K, Zhu Y, Matsushige T, Maderwald S, Umütlu L, Quick HH, Hehr U, Rath M, Ladd ME, Felbor U, Sure U. Correlation of the venous angioarchitecture of multiple cerebral cavernous malformations with familial or sporadic disease: a susceptibility-weighted imaging study with 7-Tesla MRI. *J Neurosurg* 2017; **126**: 570-577 [PMID: 27153162 DOI: 10.3171/2016.2.JNS152322]
- 41 **Moon HC**, You ST, Baek HM, Jeon YJ, Park CA, Cheong JJ, Lee YJ, Park YS. 7.0 Tesla MRI tractography in patients with trigeminal neuralgia. *Magn Reson Imaging* 2018; **54**: 265-270 [PMID: 29305127 DOI: 10.1016/j.mri.2017.12.033]
- 42 **Moon HC**, Park CA, Jeon YJ, You ST, Baek HM, Lee YJ, Cho CB, Cheong CJ, Park YS. 7 Tesla magnetic resonance imaging of caudal anterior cingulate and posterior cingulate cortex atrophy in patients with trigeminal neuralgia. *Magn Reson Imaging* 2018; **51**: 144-150 [PMID: 29777819 DOI: 10.1016/j.mri.2018.05.005]
- 43 **Hütter BO**, Altmeppen J, Kraff O, Maderwald S, Theysohn JM, Ringelstein A, Wrede KH, Dammann P, Quick HH, Schlamann M, Moeninghoff C. Higher sensitivity for traumatic cerebral microbleeds at 7 T ultra-high field MRI: is it clinically significant for the acute state of the patients and later quality of life? *Ther Adv Neurol Disord* 2020; **13**: 1756286420911295 [PMID: 32313555 DOI: 10.1177/1756286420911295]
- 44 **Chou IJ**, Lim SY, Tanasescu R, Al-Radaideh A, Mouglin OE, Tench CR, Whitehouse WP, Gowland PA, Constantinescu CS. Seven-Tesla Magnetization Transfer Imaging to Detect Multiple Sclerosis White Matter Lesions. *J Neuroimaging* 2018; **28**: 183-190 [PMID: 28944575 DOI: 10.1111/jon.12474]
- 45 **Choksi D**, Schott B, Tran K, Jang R, Hasan KM, Lincoln JA, Jalali A, Karmonik C, Salazar B, Khavari R. Disruption of specific white matter tracts is associated with neurogenic lower urinary tract dysfunction in women with multiple sclerosis. *Neurol Urodyn* 2023; **42**: 239-248 [PMID: 36321777 DOI: 10.1002/nau.25075]
- 46 **Beck ES**, Maranzano J, Luciano NJ, Parvathaneni P, Filippini S, Morrison M, Suto DJ, Wu T, van Gelderen P, de Zwart JA, Antel S, Fetco D, Ohayon J, Andrada F, Mina Y, Thomas C, Jacobson S, Duyn J, Cortese I, Narayanan S, Nair G, Sati P, Reich DS. Cortical lesion hotspots and association of subpial lesions with disability in multiple sclerosis. *Mult Scler* 2022; **28**: 1351-1363 [PMID: 35142571 DOI: 10.1177/13524585211069167]
- 47 **Voormolen EH**, Diederens SJH, Woerdeman P, van der Sprenkel JWB, Noordmans HJ, Visser F, Viergever MA, Luijten P, Hoogduin H, Robe PA. Implications of Extracranial Distortion in Ultra-High-Field Magnetic Resonance Imaging for Image-Guided Cranial Neurosurgery. *World Neurosurg* 2019; **126**: e250-e258 [PMID: 30797931 DOI: 10.1016/j.wneu.2019.02.028]
- 48 **Prener M**, Opheim G, Shams Z, Søndergaard CB, Lindberg U, Larsson HBW, Ziebell M, Larsen VA, Vestergaard MB, Paulson OB. Single-

- Voxel MR Spectroscopy of Gliomas with s-LASER at 7T. *Diagnostics (Basel)* 2023; **13** [PMID: 37238288 DOI: 10.3390/diagnostics13101805]
- 49 **Yuan Y**, Yu Y, Chang J, Chu YH, Yu W, Hsu YC, Patrick LA, Liu M, Yue Q. Convolutional neural network to predict IDH mutation status in glioma from chemical exchange saturation transfer imaging at 7 Tesla. *Front Oncol* 2023; **13**: 1134626 [PMID: 37223677 DOI: 10.3389/fonc.2023.1134626]
- 50 **Yuan Y**, Yu Y, Guo Y, Chu Y, Chang J, Hsu Y, Liebig PA, Xiong J, Yu W, Feng D, Yang B, Chen L, Wang H, Yue Q, Mao Y. Noninvasive Delineation of Glioma Infiltration with Combined 7T Chemical Exchange Saturation Transfer Imaging and MR Spectroscopy: A Diagnostic Accuracy Study. *Metabolites* 2022; **12** [PMID: 36295803 DOI: 10.3390/metabo12100901]
- 51 **Van den Boom MA**, Jansma JM, Ramsey NF. Rapid acquisition of dynamic control over DLPFC using real-time fMRI feedback. *Eur Neuropsychopharmacol* 2018; **28**: 1194-1205 [PMID: 30217551 DOI: 10.1016/j.euroneuro.2018.08.508]
- 52 **Morris LS**, Tan A, Smith DA, Grehl M, Han-Huang K, Naidich TP, Charney DS, Balchandani P, Kundu P, Murrough JW. Sub-millimeter variation in human locus coeruleus is associated with dimensional measures of psychopathology: An in vivo ultra-high field 7-Tesla MRI study. *Neuroimage Clin* 2020; **25**: 102148 [PMID: 32097890 DOI: 10.1016/j.nicl.2019.102148]
- 53 **Zoon TJC**, Mathiopoulou V, van Rooijen G, van den Munckhof P, Denys DAJP, Schuurman PR, de Bie RMA, Bot M. Apathy following deep brain stimulation in Parkinson's disease visualized by 7-Tesla MRI subthalamic network analysis. *Brain Stimul* 2023; **16**: 1289-1291 [PMID: 37619890 DOI: 10.1016/j.brs.2023.08.013]
- 54 **Alper J**, Feng R, Verma G, Rutter S, Huang KH, Xie L, Yushkevich P, Jacob Y, Brown S, Kautz M, Schneider M, Lin HM, Fleysler L, Delman BN, Hof PR, Murrough JW, Balchandani P. Stress-related reduction of hippocampal subfield volumes in major depressive disorder: A 7-Tesla study. *Front Psychiatry* 2023; **14**: 1060770 [PMID: 36816419 DOI: 10.3389/fpsy.2023.1060770]
- 55 **Prener M**, Opheim G, Simonsen HJ, Engelmann CM, Ziebell M, Carlsen J, Paulson OB. Delineation of Grade II and III Gliomas Investigated by 7T MRI: An Inter-Observer Pilot Study. *Diagnostics (Basel)* 2023; **13** [PMID: 37189466 DOI: 10.3390/diagnostics13081365]
- 56 **Weng G**, Ermiş E, Maragkou T, Krcek R, Reinhardt P, Zubak I, Schucht P, Wiest R, Slotboom J, Radojewski P. Accurate prediction of isocitrate dehydrogenase -mutation status of gliomas using SLOW-editing magnetic resonance spectroscopic imaging at 7 T MR. *Neurooncol Adv* 2023; **5**: vdad001 [PMID: 36875625 DOI: 10.1093/oaajnl/vdad001]
- 57 **Purrer V**, Upadhyay N, Borger V, Pieper CC, Kindler C, Grötz S, Keil VC, Stöcker T, Boecker H, Wüllner U. Lesions of the cerebello-thalamic tract rather than the ventral intermediate nucleus determine the outcome of focused ultrasound therapy in essential tremor: A 3T and 7T MRI-study. *Parkinsonism Relat Disord* 2021; **91**: 105-108 [PMID: 34562715 DOI: 10.1016/j.parkreldis.2021.09.013]



Published by **Baishideng Publishing Group Inc**
7041 Koll Center Parkway, Suite 160, Pleasanton, CA 94566, USA

Telephone: +1-925-3991568

E-mail: office@baishideng.com

Help Desk: <https://www.f6publishing.com/helpdesk>

<https://www.wjgnet.com>

